Macrophage Migration Inhibitory Factor Is Essential for Eosinophil Recruitment in Allergen-Induced Skin Inflammation

Yoko Yoshihisa[1,3], Teruhiko Makino[1,3], Kenji Matsunaga[1], Ayumi Honda[2], Osamu Norisugi[1], Riichiro Abe[2], Hiroshi Shimizu[2] and Tadamichi Shimizu[1]

Macrophage migration inhibitory factor (MIF) is a pluripotent cytokine that has an essential role in the pathophysiology of experimental allergic inflammation. Recent findings suggest that MIF is involved in several allergic disorders, including atopic dermatitis (AD). In this study, the role of MIF in allergic skin inflammation was examined using a murine model of AD elicited by epicutaneous sensitization with ovalbumin (OVA). We observed the number of skin-infiltrating eosinophils to significantly increase in OVA-sensitized MIF transgenic (Tg) mice compared with their wild-type (WT) littermates. On the other hand, eosinophils were virtually absent from the skin of MIF knockout (KO) mice and failed to infiltrate their skin after repeated epicutaneous sensitization with OVA. The mRNA expression levels of eotaxin and IL-5 were significantly increased in OVA-sensitized skin sites of MIF Tg mice, but were significantly decreased in MIF KO mice in comparison with the levels in WT littermates. Eotaxin expression was induced by IL-4 stimulation in fibroblasts in MIF Tg mice, but not in MIF KO mice. These findings indicate that MIF can induce eosinophil accumulation in the skin. Therefore, the targeted inhibition of MIF might be a promising new therapeutic strategy for allergic skin diseases.

Journal of Investigative Dermatology (2011) **131,** 925–931; doi:10.1038/jid.2010.418; published online 30 December 2010

INTRODUCTION

Atopic dermatitis (AD) is a chronic, relapsing inflammatory disease of the skin with significant morbidity and an adverse impact on patient well-being (Morar *et al.*, 2006). AD is considered to result from a dysregulation of the normal interactions between the environment and genes, defects in skin barrier function, and systemic and local immunological responses (Leung *et al.*, 2004). The contribution of the immune response to the pathogenesis of AD has been attributed largely to abnormalities in adaptive immunity, with key roles being played by T-helper 1(Th1)/Th2 cell dysregulation, IgE production, dendritic cell signaling, and mast-cell hyperactivity, leading to the pruritic, inflammatory dermatosis that characterizes AD (Leung *et al.*, 2004). In addition, accumulation of eosinophils is characteristic of the inflammation associated with AD (Honma *et al.*, 2000).

Macrophage migration inhibitory factor (MIF) was the first lymphokine reported to prevent random migration of macrophages (Bloom and Bennett, 1966). As the molecular cloning of MIF complementary DNA (Weiser *et al.*, 1989), MIF has been re-evaluated as a proinflammatory cytokine and pituitary-derived hormone that potentiates endotoxemia (Bernhagen *et al.*, 1993; Bucala, 1996). MIF has an important role in delayed-type hypersensitivity (Bernhagen *et al.*, 1998). Recently, it has been demonstrated that MIF also upregulates the expression of Toll-like receptor-4, which mediates lipopolysaccharide binding and activation of macrophages (Roger *et al.*, 2001). MIF is now recognized as a cytokine that exhibits a broad range of immune and inflammatory activities, including induction of inflammatory cytokines, and regulation of macrophage and lymphocyte proliferation. Furthermore, MIF induces the endothelial expression of E-selectin, ICAM-1, vascular cell adhesion molecule-1, IL-8, and monocyte chemoattractant protein-1, thus resulting in leukocyte recruitment (Gregory *et al.*, 2004, 2006; Cheng *et al.*, 2010). MIF originates from multiple cellular sources such as activated T lymphocytes, monocytes, eosinophils, and keratinocytes (Rossi *et al.*, 1998; Shimizu *et al.*, 1999; Yamaguchi *et al.*, 2000). MIF has also been shown to

[1]*Department of Dermatology, Graduate School of Medicine and Pharmaceutical Sciences, University of Toyama, Sugitani, Toyama, Japan and* [2]*Department of Dermatology, Hokkaido University Graduate School of Medicine, Sapporo, Japan*

[3]*These two authors contributed equally to this work.*

Correspondence: Teruhiko Makino or Tadamichi Shimizu, Department of Dermatology, Graduate School of Medicine and Pharmaceutical Sciences, University of Toyama, Sugitani, Toyama 930-0194, Japan.
E-mail: tmakino@med.u-toyama.ac.jp or shimizut@med.u-toyama.ac.jp

Abbreviations: AD, atopic dermatitis; KO, knockout; MIF, macrophage migration inhibitory factor; Tg, transgenic; WT, wild type

Received 9 September 2010; revised 2 November 2010; accepted 16 November 2010; published online 30 December 2010

exacerbate human allergic and inflammatory diseases, such as asthma (Rossi *et al.*, 1998) and acute respiratory distress syndrome (Donnelly *et al.*, 1997).

We recently reported excessive expression of MIF mRNA and protein in inflammatory skin lesions and in sera from AD patients (Shimizu *et al.*, 1999; Shimizu, 2005). We also showed that the serum MIF levels decrease as the clinical features of this disease improve, thus suggesting that MIF has a pivotal role in the inflammatory response in AD (Shimizu *et al.*, 1997). These studies raise the possibility that MIF is an important component of Th2-mediated immunopathology in general, and might therefore be relevant to chronic inflammatory allergic conditions.

Eosinophils may aggravate the inflammatory response in the skin of AD patients. Spergel *et al.* (1998, 1999) reported a murine model of allergic skin inflammation elicited by epicutaneous sensitization with ovalbumin (OVA). This model displays many of the features of human AD, including elevated total and specific IgE, dermatitis characterized by infiltration of the dermis by $CD4^+$ T cells and eosinophils, and increased local expression of mRNAs for the cytokines IL-4, IL-5, and IFN-γ. In our present study, MIF transgenic (Tg) mice and MIF knockout (KO) mice were used to assess the potential role of MIF in the pathogenesis of AD in this murine model of allergic skin inflammation. We also investigated the effects of MIF on eotaxin expression of dermal fibroblasts.

RESULTS

The expression of MIF was increased in bone marrow and skin from MIF Tg mice

MIF Tg mice exhibited no lethal or prominent pathological lesions in the organs examined. A northern blot analysis revealed the MIF mRNA expression in bone marrow and skin from MIF Tg mice to be ~10 times higher than that in wild-type (WT) mice (Figure 1a). MIF protein was also increased in the skin from MIF Tg mice compared with that from WT mice, as demonstrated by western blotting (Figure 1b).

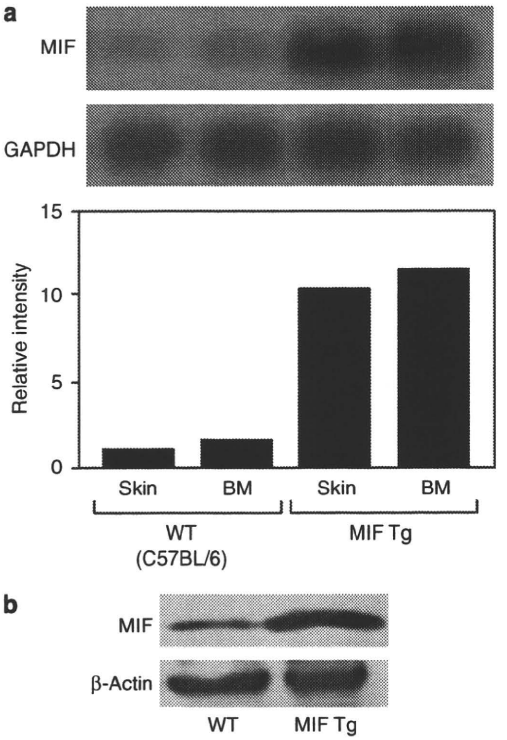

Figure 1. Expression of macrophage migration inhibitory factor (MIF) in tissues from MIF transgenic (Tg) mice. (**a**) Bone marrow (BM) and skin specimens were harvested from MIF Tg and wild-type (WT) mice, and the total RNA levels were determined by northern blot analysis as described in the Materials and Methods. The density of MIF bands was normalized to the glyceraldehyde-3-phosphate dehydrogenase (GAPDH) signals. BM and skin from MIF Tg mice showed an ~10-fold higher level of MIF mRNA expression than those from WT mice. (**b**) Western blot analysis of skin from MIF Tg mice showed that the MIF protein level was also higher in MIF Tg mice than in WT mice.

OVA-sensitized skin sites of MIF Tg mice showed marked eosinophil infiltration

To examine the role of MIF in eosinophilic infiltration, MIF Tg and WT mice were subjected to epicutaneous OVA sensitization. Only a few eosinophils were present in saline-sensitized skin from MIF Tg and WT mice, while eosinophilic infiltration of the dermis was significantly increased following epicutaneous sensitization with OVA. The mean number of eosinophils after OVA sensitization was 13.6 ± 2.84 in MIF Tg mice, but only 4.8 ± 1.37 in WT mice ($P<0.001$; Figure 2a). Figure 2b shows the histological features of OVA-sensitized skin sites in MIF Tg and WT mice. The epidermis was slightly thickened, and numerous eosinophils and mononuclear cells infiltrated the upper dermis around the vessels, in the OVA-sensitized skin of MIF Tg mice.

Eosinophil numbers were not increased in the OVA-sensitized skin of MIF KO mice

To further clarify the roles of MIF in eosinophilic infiltration, MIF KO mice were subjected to epicutaneous OVA sensitization. The mean number of eosinophils after OVA sensitization was 2.0 ± 0.94 in MIF KO mice, and did not differ from that after saline sensitization. Furthermore, this value was significantly lower than that of WT mice (4.8 ± 1.37, $P<0.05$; Figure 3a). Histological features also confirmed only a few eosinophils to be present in the dermis after OVA sensitization in MIF KO mice (Figure 3b).

The expression of eotaxin and Th2-type cytokines increased in the OVA-sensitized skin of MIF Tg mice, but decreased in the OVA-sensitized skin in MIF KO mice

We next examined the expression of mRNAs for eotaxin and cytokines in OVA-sensitized skin specimens from MIF Tg, MIF KO, and WT mice. The expression levels of eotaxin and Th2-type cytokines, especially IL-5, were increased in the OVA-sensitized skin of MIF Tg mice compared with WT mice. However, IFN-γ, a Th1-type cytokine, did not differ between MIF Tg and WT mice. Conversely, low eotaxin mRNA expression was observed in the OVA-sensitized skin of MIF KO mice compared with WT mice. Similarly, the mRNA expression of the Th2-type cytokines, including IL-4,

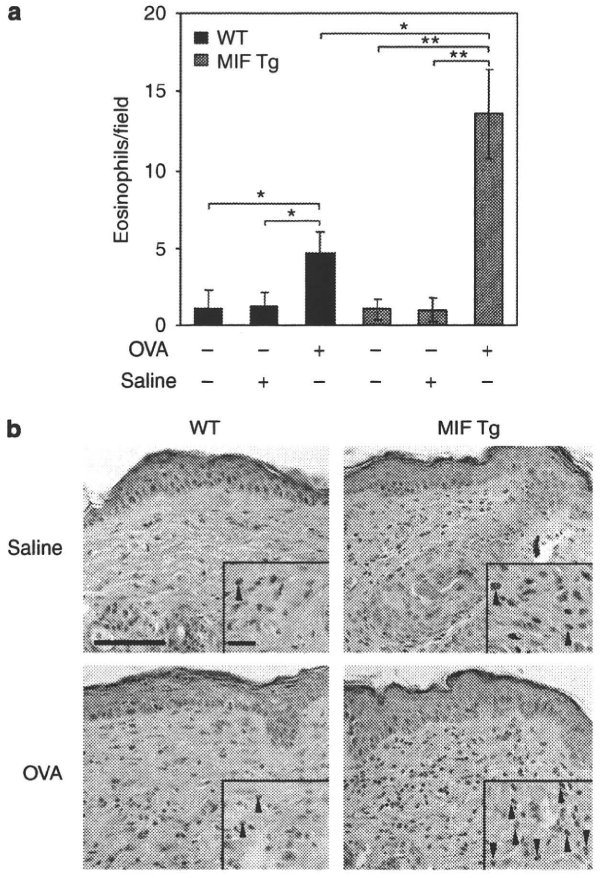

Figure 2. Eosinophil infiltration into ovalbumin (OVA)-sensitized skin sites of macrophage migration inhibitory factor (MIF) transgenic (Tg) mice. (**a**) The number of eosinophils in OVA-sensitized skin sites of MIF Tg mice was compared with the wild-type (WT) mice. Each value represents the mean ± SD ($n = 5$; $^*P < 0.001$, $^{**}P < 0.0001$). (**b**) Histological features of OVA-sensitized skin sites in MIF Tg mice and WT mice. Scale bar for large panels = 50 μm; scale bar for small panels = 10 μm; hematoxylin and eosin section. Arrowheads point to eosinophils. The experiments were repeated three times and similar results were obtained.

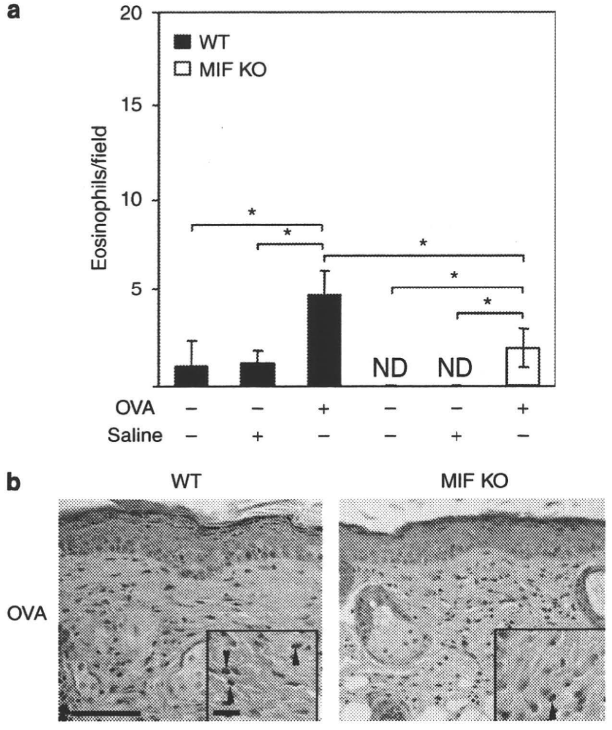

Figure 3. Eosinophil infiltration induced in ovalbumin (OVA)-sensitized skin sites of macrophage migration inhibitory factor (MIF) knockout (KO) mice. (**a**) The number of eosinophils in OVA-sensitized skin sites of MIF KO mice was compared with wild-type (WT) mice. Each value represents the mean ± SD ($n = 5$, $^*P < 0.05$). (**b**) Histological features of OVA-sensitized skin sites in MIF KO and WT mice. Scale bar for large panels = 50 μm; scale bar for small panels = 10 μm; hematoxylin and eosin section. Arrowheads point to eosinophils. The experiments were repeated three times and similar results were obtained each time.

IL-5, and IL-13, were low in the OVA-sensitized skin of MIF KO mice compared with WT mice (Figure 4).

The expression and production of eotaxin in cultured fibroblasts from MIF Tg mice and from MIF KO mice

To clarify the role of MIF in the expression of eotaxin, we performed *in vitro* experiments. A previous report described that IL-4 could dose-dependently induce the expression of eotaxin mRNA in dermal fibroblasts from humans and mice (Mochizuki *et al.*, 1998). Using this protocol, we analyzed the eotaxin expression in cultured fibroblasts from MIF Tg, MIF KO, and WT mice by stimulating them with IL-4. Unstimulated fibroblasts from these mice barely expressed eotaxin mRNA. However, fibroblasts from MIF Tg mice showed dramatically increased eotaxin mRNA after stimulation with 5 ng ml^{-1} of IL-4 (Figure 5a). To evaluate whether there was an accompanying change in eotaxin protein production, the amount of eotaxin in fibroblast supernatants was also analyzed. Eotaxin proteins in the culture supernatant of fibroblasts from MIF Tg mice were also significantly increased compared with those from WT mice ($^*P < 0.005$). However, fibroblasts from MIF KO mice showed minimal expression of eotaxin mRNA even when stimulated with 10 ng ml^{-1} of IL-4. Eotaxin production in the culture supernatant of fibroblasts from MIF KO mice was barely detectable (Figure 5b).

Recombinant MIF restored the expression and production of eotaxin in dermal fibroblasts from MIF KO mice

In dermal fibroblasts from WT mice, stimulation with IL-4 significantly induced the expression of eotaxin mRNA compared with unstimulated fibroblasts (Figure 6a). Addition of recombinant MIF significantly enhanced this increase in eotaxin expression. This suggests that the eotaxin expression in dermal fibroblasts from MIF Tg mice was markedly increased by IL-4 stimulation. A significant amount of eotaxin was also produced by combined stimulation with IL-4 ($^*P < 0.005$, $^{**}P < 0.05$; Figure 6b). Although the fibroblasts from MIF KO mice showed minimal induction of eotaxin mRNA expression in response to stimulation with IL-4, both the expression of eotaxin mRNA and the production of eotaxin protein were restored by addition of recombinant MIF

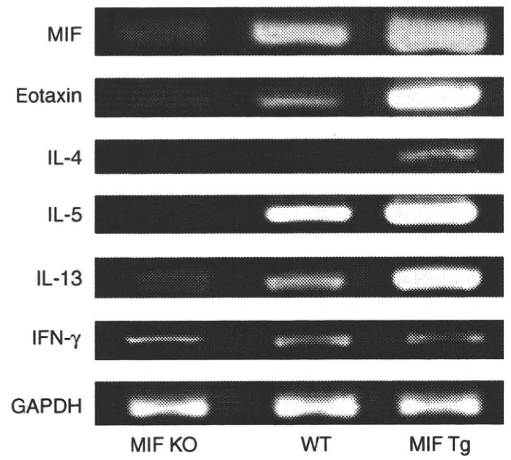

Figure 4. Expression levels of eotaxin and Th2-type cytokines in ovalbumin (OVA)-sensitized skin from macrophage migration inhibitory factor (MIF) transgenic (Tg) mice and MIF knockout (KO) mice. Reverse transcriptase-PCR analyses of eotaxin, IL-4, IL-5, IL-13, and IFN-γ levels in skin sites of MIF Tg and WT mice sensitized with OVA were performed. Eotaxin, IL-4, IL-5, and IL-13 mRNA expression levels were increased in OVA-sensitized MIF Tg; however, both eotaxin and Th2-type cytokines were markedly decreased in OVA-sensitized MIF KO mice, compared with WT mice. The experiments were repeated three times and similar results were obtained. GAPDH, glyceraldehyde-3-phosphate dehydrogenase.

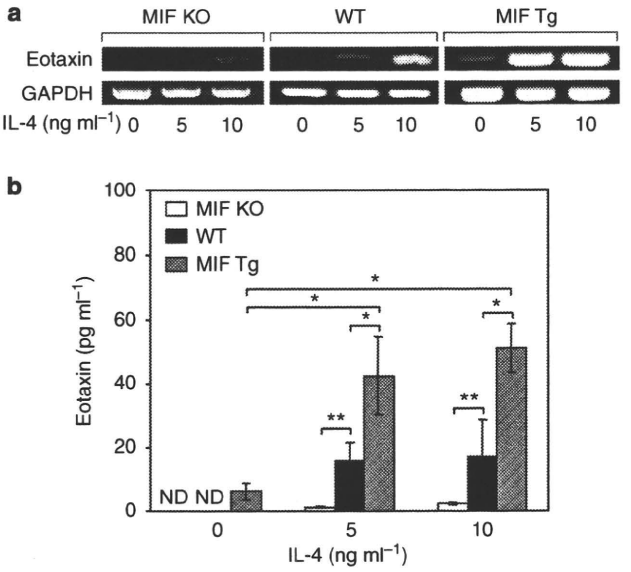

Figure 5. IL-4 induced eotaxin expression and production by fibroblasts from macrophage migration inhibitory factor (MIF) transgenic (Tg) and MIF knockout (KO) mice. Fibroblasts from MIF KO, MIF Tg, and wild-type (WT) mice were stimulated with IL-4 (5 or 10 ng ml^{-1}) for 24 hours. (**a**) RNA was extracted from the cells and the abundance of eotaxin mRNA was evaluated by reverse transcriptase-PCR. Data are from a representative experiment that was repeated three times and yielded similar results. (**b**) The eotaxin content of cultured supernatants was analyzed for eotaxin by ELISA. Each value represents the mean ± SD of five specimens. *P<0.005, **P<0.05. ND, not detected.

(Figure 6a and b). The levels of eotaxin production in MIF KO mouse fibroblasts exposed to MIF were similar to the levels in WT fibroblasts stimulated with IL-4 (Figure 6b).

DISCUSSION

There is growing evidence that the eosinophil is an important effecter cell in allergic inflammatory diseases, such as asthma and AD. Accumulation of eosinophils in the skin is characteristic of inflammation associated with AD (Leiferman, 1989; Kapp, 1995). This study explored, for the first time, the significant increase in eosinophil infiltration in the skin of MIF Tg mice after OVA sensitization, compared with WT mice. However, in MIF KO mice, eosinophils failed to infiltrate the skin after repeated epicutaneous sensitization with OVA. Eosinophils accumulate at inflammatory sites and release numerous mediators capable of initiating and maintaining allergic inflammation. Yamaguchi *et al.* (2000) reported eosinophils to be an important source of MIF in allergic inflammatory diseases. The number of eosinophils was reported to be significantly decreased in lung tissue and in bronchoalveolar lavage fluid from MIF KO mice after stimulation with OVA, compared with those from WT mice (Mizue *et al.*, 2005; Magalhães *et al.*, 2007; Wang *et al.*, 2009). In an allergic rhinitis model, eosinophil recruitment into the nasal submucosa was also suppressed in MIF KO mice (Nakamaru *et al.*, 2005). Consistent with these findings, our current evidence indicates that MIF is essential for the infiltration of eosinophils into the OVA-sensitized skin.

This study also demonstrated that the expression of both eotaxin and IL-5 is markedly increased in the OVA-sensitized

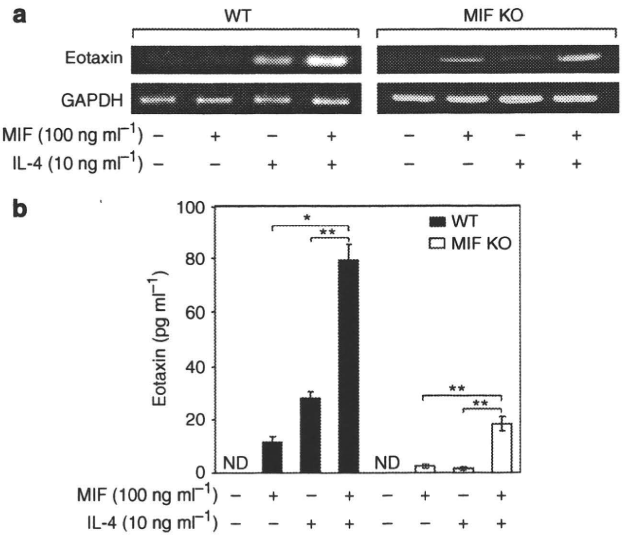

Figure 6. Recombinant macrophage migration inhibitory factor (MIF) restored eotaxin expression and production by IL-4 stimulation in dermal fibroblasts from MIF knockout (KO) mice. The fibroblasts were stimulated with IL-4 (10 ng ml^{-1}), MIF (100 ng ml^{-1}), or both IL-4 and MIF for 24 hours. (**a**) RNA was extracted from cells, and the abundance of eotaxin mRNA was evaluated by reverse transcriptase-PCR. Data are from a representative experiment that was repeated three times showing similar results. (**b**) The eotaxin contents of cultured supernatants were analyzed for eotaxin by ELISA. Each value represents the mean ± SD of six specimens. *P<0.005, **P<0.05. GAPDH, glyceraldehyde-3-phosphate dehydrogenase; ND, not detected.

skin sites of MIF Tg mice skin. The other Th2-type cytokines, IL-4 and IL-13, were also slightly increased in MIF Tg mice. On the other hand, the expression levels of eotaxin and Th2-type cytokines were markedly decreased in the OVA-sensitized skin sites of MIF KO mice. Acute AD involves a systemic Th2 response with eosinophilia, and marked infiltration of Th2 cells into skin lesions. These infiltrating T cells predominantly express IL-4, IL-5, and IL-13. Furthermore, the roles of cytokines in the induction of migration and the accumulation of eosinophils into an inflamed tissue have been extensively studied in recent years. Some of the important eosinophil chemoattractant cytokines include IL-5, IL-8, eotaxin, RANTES (regulated on activation, normal T cell expressed and secreted), and monocyte chemoattractant protein-3 (Lampinen *et al.*, 2004). Among these, eotaxin (CC chemokine ligand-11) is one of the most important eosinophil-selective chemoattractants (Jose *et al.*, 1994; Garcia-Zepeda *et al.*, 1996). Eotaxin is secreted by several cell types: epithelial cells, fibroblasts, and activated infiltrating leukocytes such as eosinophils (Garcia-Zepeda *et al.*, 1996; Ponath *et al.*, 1996; Uguccioni *et al.*, 1996). Eotaxin is reportedly related to the eosinophilia in allergic diseases, including AD and asthma (Ying *et al.*, 1997; Yawalkar *et al.*, 1999). IL-5 also has an important role in eosinophil development and differentiation (Sanderson, 1992). IL-5 KO mice had virtually no eosinophils in either saline-sensitized skin or in OVA-sensitized skin (Spergel *et al.*, 1999). Recently, Magalhães *et al.* (2009) reported that MIF was involved in IL-5-driven maturation of eosinophils and in tissue eosinophilia associated with *Schistosoma mansoni* infection. In addition, several earlier studies demonstrated that MIF KO mice failed to develop tissue eosinophilia, and that eotaxin, IL-4, and IL-5 were not induced in either allergic lung tissues or bronchoalveolar lavage fluid (Mizue *et al.*, 2005; Wang *et al.*, 2006). Accordingly, our results suggest that MIF is important in regulating both eotaxin and IL-5 in OVA-sensitized inflamed skin tissue.

In support of these *in vivo* observations, this study demonstrated that the expression of eotaxin was significantly increased after stimulation with IL-4 in fibroblasts from MIF Tg mice compared with WT fibroblasts, but not in fibroblasts from MIF KO mice. However, eotaxin expression in fibroblasts from MIF KO mice was restored by addition of recombinant MIF. These observations suggest that MIF is crucial to the expression of eotaxin, and antigen-induced eosinophil infiltration is suspected to be induced by eotaxin mainly by MIF, in addition with IL-5 production involved in MIF. Previous observations have shown that either IL-4 or IL-13 can increase eotaxin expression, and that they function synergistically with proinflammatory cytokines, such as tumor necrosis factor-α, to increase the production of eotaxin in epithelial cells and fibroblasts (Mochizuki *et al.*, 1998; Nakamura *et al.*, 1998; Li *et al.*, 1999; Stellato *et al.*, 1999; Fujisawa *et al.*, 2000; Terada *et al.*, 2000). Increases in both IL-4 and IL-13 in the inflamed skin of MIF Tg mice might involve enhancing the tissue eosinophilia. Furthermore, tumor necrosis factor-α secretion induced by MIF also has the ability to increase eotaxin expression in MIF Tg mice, on the basis of the known capacity of MIF to trigger the secretion of several inflammatory cytokines, including tumor necrosis factor-α (Donnelly *et al.*, 1997). It was recently elucidated that MIF activates an extracellular signal-regulated kinase-1/2–mitogen-activated protein kinase signaling through its receptor CD74 (Leng *et al.*, 2003) and c-Jun N-terminus kinase–mitogen-activated protein kinase signaling through CD74/CXCR4 (Lue *et al.*, 2011), in addition to the endocytic pathway described previously (Kleemann *et al.*, 2000); however, the receptor-mediated mechanism involved in MIF-mediated IL-4-induced eotaxin release is unclear. This mechanism should therefore be an important focus of research in association with MIF-mediated skin allergy.

Finally, we suggest that the inhibition of MIF might be an effective treatment for AD, suppressing both eosinophil infiltration and eotaxin expression in the skin. We recently demonstrated that in murine models of AD, MIF–DNA vaccination elicited the production of endogenous anti-MIF antibodies, producing rapid improvement of AD skin manifestations (Hamasaka *et al.*, 2009). Our previous data and the current findings therefore hold promise for the development of MIF inhibitors as a therapeutic strategy for allergic diseases.

MATERIALS AND METHODS

Materials

The following materials were obtained from commercial sources: a mouse eotaxin-specific ELISA kit from Genzyme TECHNE (Cambridge, MT); Isogen RNA extraction kit from Nippon Gene (Tokyo, Japan); M-MLV reverse transcriptase from GIBCO (Grand Island, NY); Taq DNA polymerase from Perkin-Elmer (Norwalk, CO); nylon membranes from Schleicher & Schuell (Keene, NH); Ficoll-Plaque Plus and Protein A Sepharose from Pharmacia (Uppsala, Sweden); recombinant mouse IL-4 from R&D systems (Minneapolis, MN). Recombinant rat MIF (this recombinant MIF crossreacts with that of mice) was expressed in *Escherichia coli* BL21/DE3 (Novagen, Madison, WI) and was purified as described previously (Shimizu *et al.*, 2004). All other chemicals were of analytical grade.

Mice

The MIF-overexpressing Tg mice were established after complementary DNA microinjection. Physical and biochemical characteristics, including body weight, blood pressure, and serum cholesterol and blood sugar levels, were normal, as reported previously (Sasaki *et al.*, 2004). The transgene expression was regulated by a hybrid promoter composed of the cytomegalovirus enhancer and the β-actin/β-globin promoter, as reported previously (Akagi *et al.*, 1997). The strain of the original MIF Tg mice was ICR, which were backcrossed with C57BL/6 for at least 10 generations. Tg mice were maintained by heterozygous sibling mating. Aged MIF Tg mice of 12 months or older developed neither skin allergies nor diseases. The MIF-deficient (KO) mice were established by targeted disruption of the *MIF* gene as described previously (Honma *et al.*, 2000), using a mouse strain bred onto a C57BL/6 background. MIF Tg, MIF KO, and WT mice were maintained under specific-pathogen-free conditions at the Institute for Animal Experiments of the Graduate School of Medicine and Pharmaceutical Sciences, University of Toyama. All experiments were performed on 8-week-old female adult mice.

Epicutaneous sensitization

Epicutaneous sensitization of mice was performed as described previously (Spergel *et al.*, 1998). Briefly, each mouse was anesthetized with 10% nembutal (Hospira, Osaka, Japan), then shaved with a razor. One hundred mg of OVA (Sigma, St Louis, MO) in 100 μl of normal saline were placed on a 1 × 1 cm patch (Alcare, Tokyo, Japan), which was secured to the skin with a transparent bio-occlusive dressing (ALCARE). The patch was left in place for 1 week and then removed. At the end of the second week, an identical patch was reapplied to the same skin site. Each mouse had a total of three 1-week exposures to the patch, separated from each other by 2-week intervals. Inspection confirmed that the patch was still in place at the end of each sensitization period. Skin biopsies from treated areas were obtained for RNA isolation and histological evaluation. Six-micrometer thick skin sections were stained with hematoxylin and eosin (H&E). Eosinophils were counted under a microscope at a magnification of × 400 and expressed as the mean number of the cells in five random fields (one section per mouse, five mice per group).

Northern blot analysis

Bone marrow cells were isolated from the femurs of MIF Tg or WT mice, and 1×10^6 cells ml^{-1} was collected. Total RNA was isolated from bone marrow cells and skin from mice using an Isogen RNA extraction kit according to the manufacturer's protocols. Twenty μg of RNA from control and test samples were loaded onto a formaldehyde-agarose gel and the RNA was transferred onto a nylon membrane. RNA fragments obtained by restriction enzyme treatment for MIF and glyceraldehyde-3-phosphate dehydrogenase were labeled with [α-^{32}P]deoxycytidine triphosphate using a DNA random primer labeling kit (Enzo Life Sciences International, Farmingdale, NY). Hybridization was carried out at 42 °C for 24–48 hours. Post-hybridization washing was performed in 0.1% SDS with 0.2 × standard saline citrate (1 × standard saline citrate: 0.15 M NaCl, 0.015 M sodium citrate) at 65 °C for 15 minutes. The radioactive bands were visualized by autoradiography on Kodak X-AR5 film (Tokyo, Japan) and quantitatively analyzed using the NIH Image system (Bethesda, MD). The results were normalized by compensating for the glyceraldehyde-3-phosphate dehydrogenase mRNA levels.

Reverse transcription-PCR analysis

Total RNA was extracted from each mouse skin specimen. RNA reverse transcription was performed with M-MLV reverse transcriptase using random hexamer primers and subsequent amplification using Taq DNA polymerase. PCR was carried out for 35–40 cycles with denaturation at 94 °C for 30 seconds, annealing from 46 to 64 °C for 1 minute and extension at 72 °C for 45 seconds using a thermal cycler (PE Applied Biosystems Gene Amp PCR system 9700, Life Technologies Japan, Tokyo, Japan). The primers used in this study are described in Supplementary Table S1 online. After PCR, the amplified products were analyzed by 2% agarose gel electrophoresis.

Western blot analysis

The epidermis of each mouse was homogenized with a Polytron homogenizer (Kinematica, Lausanne, Switzerland). The protein concentrations of the cell homogenates were quantified using a Micro BCA protein assay reagent kit (Thermo Fisher Scientific, Yokohama, Japan). Equal amounts of homogenates were dissolved in 20 μl of Tris-HCL, 50 mM (pH 6.8), containing 2-mercaptoethanol (1%), SDS (2%), glycerol (20%) and bromophenol blue (0.04%), and then were heated to 100 °C for 5 minutes. The samples were then subjected to SDS-PAGE and electrophoretically transferred onto a nitrocellulose membrane. The membranes were blocked with 2.5% non-fat dry milk powder in phosphate-buffered saline, probed with antibodies against MIF (Shimizu *et al.*, 1996) and subsequently reacted with secondary IgG antibodies coupled with horseradish peroxidase. The resultant complexes were processed for the ECL detection system (Amersham Biosciences, Buckinghamshire, UK). The relative amounts of proteins associated with specific antibodies were normalized according to the intensities of β-actin (Sigma).

Cell culture

Skin specimens were obtained from the dorsal surfaces of newborn MIF Tg, MIF KO, and WT mice. The skin specimens were cut into 3–5 mm pieces and placed on a large Petri dish with the subcutaneous side down, followed by tissue incubation for 1 week in a humidified atmosphere of 5% CO_2 at 37 °C. Once sufficient numbers of fibroblasts had migrated out of the skin sections, pieces of the skin were removed and the cells were passaged by trypsin digestion in the same manner as wound-harvested fibroblasts. Fibroblasts were grown in DMEM containing 10% fetal calf serum and 1% penicillin/streptomycin. After 3 passages, the fibroblasts were used for the experiments. The fibroblasts from MIF KO and WT mice were stimulated with MIF (100 ng ml^{-1}), IL-4 (10 ng ml^{-1}), or MIF (100 ng ml^{-1}) in combination with IL-4 (10 ng ml^{-1}) for 24 hours. We also stimulated the fibroblasts from MIF Tg, MIF KO, and WT mice with IL-4 (5 or 10 ng ml^{-1}) alone for 24 hours. The cells were analyzed using reverse transcriptase-PCR. Culture supernatants were analyzed for eotaxin by ELISA.

Statistical analysis

Values are expressed as the means ± SD of the respective test or control group. The statistical significance of differences between the control and test groups was evaluated by either Student's *t*-test or one-way analysis of variance.

CONFLICT OF INTEREST

The authors state no conflict of interest.

ACKNOWLEDGMENTS

This research was supported by a Grant-in-Aid for Scientific Research (Nos.11670813 and 13357008) from the Japan Society for the Promotion of Science.

SUPPLEMENTARY MATERIAL

Supplementary material is linked to the online version of the paper at http://www.nature.com/jid

REFERENCES

Akagi Y, Isaka Y, Akagi A *et al.* (1997) Transcriptional activation of a hybrid promoter composed of cytomegalovirus enhancer and beta-actin/beta-globin gene in glomerular epithelial cells *in vivo*. *Kidney Int* 51:1265–9

Bernhagen J, Calandra T, Bucala R (1998) Regulation of the immune response by macrophage migration inhibitory factor: biological and structural features. *J Mol Med* 76:151–61

Bernhagen J, Calandra T, Mitchell RA *et al.* (1993) MIF is a pituitary-derived cytokine that potentiates lethal endotoxaemia. *Nature* 365:756–9

Bloom BR, Bennett B (1966) Mechanism of reaction *in vivo* associated with delayed-type hypersensitivity. *Science* 153:80–2

Bucala R (1996) MIF re-evaluated: pituitary hormone and glucocorticoid-induced regulator of cytokine production. *FASEB J* 7:19–24

Cheng Q, McKeown SJ, Santos L *et al.* (2010) Macrophage migration inhibitory factor increases leukocyte-endothelial interactions in human endothelial cells via promotion of expression of adhesion molecules. *J Immunol* 185:1238–47

Donnelly SC, Haslett C, Reid PT *et al.* (1997) Regulatory role for macrophage migration Inhibitory factor in acute respiratory distress syndrome. *Nat Med* 3:320–3

Fujisawa T, Kato Y, Atsuta J *et al.* (2000) Chemokine production by the BEAS-2B human bronchial epithelial cells: differential regulation of eotaxin, IL-8, and RANTES by TH2- and TH1-derived cytokines. *J Allergy Clin Immunol* 105:126–33

Garcia-Zepeda EA, Rothenberg ME, Ownbey RT *et al.* (1996) Human eotaxin is a specific chemoattractant for eosinophil cells and provides a new mechanism to explain tissue eosinophilia. *Nat Med* 2:449–56

Gregory JL, Leech MT, David JR *et al.* (2004) Reduced leukocyte-endothelial cell interactions in the inflamed microcirculation of macrophage migration inhibitory factor-deficient mice. *Arthritis Rheum* 50:3023–34

Gregory JL, Morand EF, McKeown SJ *et al.* (2006) Macrophage migration inhibitory factor induces macrophage recruitment via CC chemokine ligand 2. *J Immunol* 177:8072–9

Hamasaka A, Abe R, Koyama Y *et al.* (2009) DNA vaccination against macrophage migration inhibitory factor improves atopic dermatitis in murine models. *J Allergy Clin Immunol* 124:90–9

Honma N, Koseki H, Akasaka T *et al.* (2000) Deficiency of the macrophage migration inhibitory factor gene has no significant effect on endotoxaemia. *Immunology* 100:84–90

Jose PJ, Griffiths-Johnson DA, Collins PD *et al.* (1994) Eotaxin: a potent eosinophil chemoattractant cytokine detected in a guinea pig model of allergic airways inflammation. *J Exp Med* 179:881–7

Kapp A (1995) Atopic dermatitis-the skin manifestation of atopy. *Clin Exp Allergy* 25:210–9

Kleemann R, Hausser A, Geiger R *et al.* (2000) Intracellular action of the cytokine MIF to modulate AP-1 activity and the cell cycle through Jab1. *Nature* 408:211–6

Lampinen M, Carlson M, Hakansson LD *et al.* (2004) Cytokine-regulated accumulation of eosinophils in inflammatory disease. *Allergy* 59:793–805

Leiferman KM (1989) Eosinophils in atopic dermatitis. *Allergy* 44:20–6

Leng L, Metz CN, Fang Y *et al.* (2003) MIF signal transduction initiated by binding to CD74. *J Exp Med* 197:1467–76

Leung DY, Nicklas RA, Li JT *et al.* (2004) Disease management of atopic dermatitis: an updated practice parameter. Joint Task Force on Practice Parameters. *Ann Allergy Asthma Immunol* 93:S1–21

Li L, Xia Y, Nguyen A *et al.* (1999) Effects of Th2 cytokines on chemokine expression in the lung: IL-13 potently induces eotaxin expression by airway epithelial cells. *J Immunol* 162:2477–87

Lue H, Dewor M, Leng L *et al.* (2011) Activation of the JNK signaling pathway by macrophage migration inhibitory factor (MIF) and dependence on CXCR4 and CD74. *Cell Signal* 23:135–44

Magalhães ES, Mourao-Sa DS, Vieira-de-Abreu A *et al.* (2007) Macrophage migration inhibitory factor is essential for allergic asthma but not for Th2 differentiation. *Eur J Immunol* 37:1097–106

Magalhães ES, Paiva CN, Souza HS *et al.* (2009) Macrophage migration inhibitory factor is critical to interleukin-5-driven eosinophilopoiesis and tissue eosinophilia triggered by Schistosoma mansoni infecton. *FASEB J* 23:1262–71

Mizue Y, Ghani S, Leng L *et al.* (2005) Role for macrophage migration inhibitory factor in asthma. *Proc Natl Acad Sci USA* 102:14410–5

Mochizuki M, Bartels J, Mallet AI *et al.* (1998) IL-4 induces eotaxin: a possible mechanism of selective eosinophil recruitment in helminth infection and atopy. *J Immunol* 160:60–8

Morar N, Willis-Owen SA, Moffatt MF *et al.* (2006) The genetics of atopic dermatitis. *J Allergy Clin Immunol* 118:24–34

Nakamaru Y, Oridate N, Nishihira J *et al.* (2005) Macrophage migration inhibitory factor (MIF) contributes to the development of allergic rhinitis. *Cytokine* 31:103–8

Nakamura H, Haley KJ, Nakamura T *et al.* (1998) Differential regulation of eotaxin expression by TNF-alpha and PMA in human monocytic U-937 cells. *Am J Physiol* 275:L601–10

Ponath PD, Qin S, Post TW *et al.* (1996) Molecular cloning and characterization of a human eotaxin receptor expressed selectively on eosinophils. *J Exp Med* 183:2437–48

Roger T, David J, Glauser MP *et al.* (2001) MIF regulates innate immune responses through modulation of Toll-like receptor 4. *Nature* 414:920–4

Rossi AG, Haslett C, Hirani N *et al.* (1998) Human circulating eosinophils secrete macrophage migration inhibitory factor (MIF): potential role in asthma. *J Clin Invest* 15:2869–74

Sanderson CJ (1992) Interleukin-5, eosinophils, and disease. *Blood* 79:3101–9

Sasaki S, Nishihira J, Ishibashi T *et al.* (2004) Transgene of MIF induces podocyte injury and progressive mesangial sclerosis in the mouse kidney. *Kidney Int* 65:469–81

Shimizu T (2005) Role of macrophage migration inhibitory factor (MIF) in the skin. *J Dermatol Sci* 37:65–73

Shimizu T, Abe R, Ohkawara A *et al.* (1997) Macrophage migration inhibitory factor is an essential immunoregulatory cytokine in atopic dermatitis. *Biochem Biophy Res Commun* 240:173–8

Shimizu T, Abe R, Ohkawara A *et al.* (1999) Increased production of macrophage migration inhibitory factor (MIF) by PBMCs of atopic dermatitis. *J Allergy Clin Immunol* 104:659–64

Shimizu T, Nishihira J, Watanabe H *et al.* (2004) Cetirizine, an H1-receptor antagonist, suppresses the expression of macrophage migration inhibitory factor (MIF): its potential anti-inflammatory action. *Clin Exp Allergy* 34:103–9

Shimizu T, Ohkawara A, Nishihira J *et al.* (1996) Identification of macrophage migration inhibitory factor (MIF) in human skin and its immunohistochemical localization. *FEBS Lett* 381:188–202

Spergel JM, Mizoguchi E, Brewer JP *et al.* (1998) Epicutaneous sensitization with protein antigen induces localized allergic dermatitis and hyperresponsiveness to methacholine after single exposure to aerosolized antigen in mice. *J Clin Invest* 101:1614–22

Spergel JM, Mizoguchi E, Oettgen H *et al.* (1999) Roles of TH1 and TH2 cytokines in a murine model of allergic dermatitis. *J Clin Invest* 103:1103–11

Stellato C, Matsukura S, Fal A *et al.* (1999) Differential regulation of epithelial-derived C-C chemokine expression by IL-4 and glucocorticoid budesonide. *J Immunol* 163:5624–32

Terada N, Hamano N, Nomura T *et al.* (2000) Interleukin-13 and tumor necrosis factor-a synergistically induce eotaxin production in human nasal fibroblasts. *Clin Exp Allergy* 20:348–55

Uguccioni M, Loetscher P, Forssmann U *et al.* (1996) Monocyte chemotactic protein 4 (MCP-4), a novel structural and functional analogue of MCP-3 and eotaxin. *J Exp Med* 183:2379–84

Wang B, Huang X, Wolters PJ *et al.* (2006) Cutting edge: deficiency of macrophage migration inhibitory factor impairs murine airway allergic responses. *J Immunol* 177:5779–84

Wang B, Zhang Z, Wang Y *et al.* (2009) Molecular cloning and characterization of macrophage migration inhibitory factor from small abalone Haliotis diversicolor supertexta. *Fish Shellfish Immunol* 27:57–64

Weiser WY, Temple PA, Witek-Giannotti JS *et al.* (1989) Molecular cloning of a cDNA encoding a human macrophage migration inhibitory factor. *Proc Natl Acad Sci USA* 86:7522–6

Yamaguchi E, Nishihira J, Shimizu T *et al.* (2000) Macrophage migration inhibitory factor (MIF) in bronchial asthma. *Clin Exp Allergy* 30:1244–9

Yawalkar N, Uguccioni M, Schärer J *et al.* (1999) Enhanced expression of eotaxin and CCR3 in atopic dermatitis. *J invest Dermatol* 113:43–8

Ying S, Robinson DS, Meng Q *et al.* (1997) Enhanced expression of eotaxin and CCR3 mRNA and protein in atopic athma. Association with airway hyperresponsiveness and predominant co-localization of eotaxin mRNA to bronchial epithelial and endothelial cells. *Eur J Immunol* 27:3507–16

MUTATION UPDATE

Human Mutation

OFFICIAL JOURNAL
HGVS
HUMAN GENOME VARIATION SOCIETY
www.hgvs.org

ABCA12 Mutations and Autosomal Recessive Congenital Ichthyosis: A Review of Genotype/Phenotype Correlations and of Pathogenetic Concepts

Masashi Akiyama*

Department of Dermatology, Hokkaido University Graduate School of Medicine, Sapporo, Japan

Communicated by Mark H. Paalman

Received 17 March 2010; accepted revised manuscript 7 July 2010.
Published online 29 July 2010 in Wiley Online Library (wileyonlinelibrary.com). DOI 10.1002/humu.21326

ABSTRACT: Mutations in *ABCA12* have been described in autosomal recessive congenital ichthyoses (ARCI) including harlequin ichthyosis (HI), congenital ichthyosiform erythroderma (CIE), and lamellar ichthyosis (LI). HI shows the most severe phenotype. CIE and LI are clinically characterized by fine, whitish scales on a background of erythematous skin, and large, thick, dark scales over the entire body without serious background erythroderma, respectively. To date, a total of 56 *ABCA12* mutations have been reported in 66 ARCI families including 48 HI, 10 LI, and 8 CIE families of African, European, Pakistani/Indian, and Japanese origin (online database: http://www.derm-hokudai.jp/ABCA12/). A total of 62.5% of reported *ABCA12* mutations are expected to lead to truncated proteins. Most mutations in HI are truncation mutations and homozygous or compound heterozygous truncation mutations always results in HI phenotype. In CIE families, at least one mutation on each allele is typically a missense mutation. Combinations of missense mutations in the first ATP-binding cassette of ABCA12 underlie the LI phenotype. ABCA12 is a keratinocyte lipid transporter associated with lipid transport in lamellar granules, and loss of ABCA12 function leads to a defective lipid barrier in the stratum corneum, resulting in an ichthyotic phenotype. Recent work using mouse models confirmed ABCA12 roles in skin barrier formation.
Hum Mutat 31:1090–1096, 2010. © 2010 Wiley-Liss, Inc.

KEY WORDS: ABCA12; congenital ichthyosiform erythroderma; harlequin ichthyosis; lamellar ichthyosis

Introduction

Severe autosomal recessive congenital ichthyoses (ARCI) can be devastating to patients' quality of life in those seriously affected, even though other organs are uninvolved. ARCI comprises three major subtypes, harlequin ichthyosis (HI; MIM# 242500), congenital ichthyosiform erythroderma (CIE; MIM# 242100), and lamellar ichthyosis (LI; MIM#s 242300, 604777, 601277, 606545) [Akiyama and Shimizu, 2008]. HI is the most devastating congenital ichthyosis, and affected newborns show large, thick, plate-like scales over the whole body with severe ectropion, eclabium, and flattened ears [Akiyama, 2006a]. Patients with CIE demonstrate fine, whitish scales on a background of erythematous skin over the whole body. Conversely, LI is clinically characterized by large, thick, dark scales over the entire body surface without a serious background erythroderma [Akiyama et al., 2003].

Because transglutaminase 1 gene (*TGM1*; MIM# 190195) mutations were identified as the cause in LI in 1995 [Huber et al., 1995; Russell et al., 1995], significant progress has recently been made in the understanding of the molecular basis of the human epidermal keratinization processes, and mutations in several other genes have also been identified in ARCI. In HI cases, only ABCA12 mutations have been reported as underlying genetic defects [Akiyama and Shimizu, 2008]. In contrast, CIE and LI are both heterogeneous genetic disorders and several causative or underlying molecules including ABCA12 have been identified [Jobard et al., 2002; Lefèvre et al., 2003, 2004; Lefèvre, 2006]. Mutations in six genes have been described in non-HI ARCI to date, including *TGM1* [Huber et al., 1995; Russell et al., 1995], *ABCA12* [Lefèvre et al., 2003; Natsuga et al., 2007], *NIPAL4* (also known as *ICHTHYIN*) [Lefèvre et al., 2004], *CYP4F22* [Lefèvre, 2006], *ALOX12B* and *ALOXE3* [Jobard et al., 2002]. Among them, *TGM1* is thought to be the most prevalent causative gene [Fischer, 2009; Herman et al., 2009]. *TGM1* encodes transglutaminase 1, which is expressed in the upper epidermis and catalyzes crosslinking of cornified cell envelope precursor proteins to form a cornified cell envelope in the stratum corneum [Herman et al., 2009]. *NIPAL4* (or *ICHTHYIN*) encodes a protein of unknown function. ALOX12B and ALOXE3 encode for arachidonate 12(R)-lipoxygenase and arachidonate lipoxygenase-3, respectively. The protein product of CYP4F22, a cytochrome P450 protein, and the two lipoxygenases arachidonate 12(R)-lipoxygenase and arachidonate lipoxygenase-3 are part of the lipid metabolism pathway involved in the formation of ω-hydroxyceramides from arachidonic acid [Brash et al., 2007]. ABCA12 (MIM# 607800) missense mutations leading to defects in the ATP-binding cassette were reported in LI cases (type 2 LI [MIM# 601277]) [Lefèvre et al., 2003] and ABCA12 truncation mutations were reported underlying HI patients [Akiyama et al., 2005; Kelsell et al., 2005]. Recently, we reported that *ABCA12* missense mutations are a major cause of CIE cases in the Japanese population [Akiyama et al., 2008; Natsuga et al., 2007; Sakai et al., 2009]. Thus, *ABCA12* mutations lead to all three ARCI clinical phenotypes including HI, LI and CIE and *ABCA12* mutations are highlighted as one of the major causes of ARCI.

Additional Supporting Information may be found in the online version of this article.

*Correspondence to: Masashi Akiyama, Department of Dermatology, Hokkaido University Graduate School of Medicine, North 15 West 7, Sapporo 060-8638, Japan. E-mail: akiyama@med.hokudai.ac.jp

ABCA12 is a member of the large superfamily of the ATP-binding cassette (ABC) transporters [Annilo et al., 2002], which bind and hydrolyze ATP to transport various molecules across a limiting membrane or into a vesicle [Borst and Elferink, 2002]. The ABCA subfamily members are thought to be lipid transporters [Peelman et al., 2003]. ABCA12 was recognized as a key molecule in keratinocyte lipid transport [Akiyama et al., 2005; Sakai et al., 2007]. ABCA12 is a keratinocyte transmembrane lipid transporter protein associated with lipid transport in lamellar granules to the apical surface of granular layer keratinocytes [Akiyama et al., 2005]. In this article, the importance of *ABCA12* mutations as a cause for ARCI is reviewed and a genotype/phenotype correlation of ARCI with *ABCA12* mutations is discussed.

ABCA12 Mutations

A review of the literature was performed to identify all of the known *ABCA12* mutations. To date, 56 *ABCA12* mutations have been described (online database: http://www.derm-hokudai.jp/ABCA12/) in 66 unrelated families including 48 HI, 10 LI and 8 CIE families (Supp. Table S1 and Fig. 1). Nucleotide numbering reflects cDNA numbering with +1 corresponding to the A of the ATG translation initiation codon in the reference sequence (GenBank NM_173076.2), according to journal guidelines (www.hgvs.org/mutnomen). The initiation codon is codon 1. Mutations have been reported among ARCI patients with African, European, Pakistani/Indian, and Japanese backgrounds, from almost all over the world. Of the 56 mutations, 36% (20) are nonsense, 25% (14) are missense, 20% (11) comprise small deletions, 11% (6) are splice site, 5% (3) are large deletions, and 4% (2) are insertion mutations. At least, 62.5% (35) of the total reported mutations are predicted to result in truncated proteins. There is no apparent mutation hot spot in *ABCA12*, although mutations underlying LI phenotype are clustered in the region of the first ATP-binding cassette [Lefèvre et al., 2003].

The most common reported mutation in *ABCA12* is c.7322delC (p.Val2442SerfsTer28) in exon 49, which has been reported in seven HI families with Pakistani background [Kelsell et al., 2005; Thomas et al., 2006, 2008]. This mutation has been identified only in the Pakistani population. Thomas et al. [2008] reported that 80% of HI patients and parents (10 screened) originated from the Pakistani/Indian area had the mutation 7322delC. Microsatellite-based haplotype analysis of the genomic region harboring *ABCA12* in three patients homozygous for the mutation c.7322delC suggested that c.7322delC is a possible founder mutation in the Pakistani population [Thomas et al., 2008]. The second most common reported *ABCA12* mutation is a missense mutation p.Asn1380Ser in Walker A motif of the first ATP-binding cassette, which is essential for the transporter function of ABCA12 [Lefèvre et al., 2003]. This missense mutation p.Asn1380Ser has been identified in five LI families from Africa (three families from Morocco and two families from Algeria) [Lefèvre et al., 2003]. Haplotype analysis confirmed that p.Asn1380Ser is a founder mutation in the patients from Morocco/Algeria region [Lefèvre et al., 2003]. Out of further 10 different *ABCA12* mutations, each mutation has been identified in two unrelated families from certain geographic regions. Among these 10 mutations, 5 *ABCA12* mutations, c.2021_2022del2, c.3295−2A>G, p.Thr1387del, p.Arg1950Ter, and p.Arg2482Ter, were found in two independent patients from Japan [Akiyama et al., 2005, 2006a, 2007a; Sakai et al., 2009]. As for the other five mutations, p.Trp1294Ter, p.Gly1651Ser, p.Tyr1090Ter, c.2025delG, and p.Trp1744Ter were found in two independent families with Pakistani [Rajpar et al., 2006; Thomas et al., 2006], Algeria [Lefèvre et al., 2003], Albanian/Bosnian [Thomas et al., 2008], Anglo-Saxon [Thomas et al., 2006], and native American [Kelsell et al., 2005] origins, respectively. These data suggest the presence of founder mutations in patients in Pakistani/Indian, African, European, and Japanese origins.

Clinical Significance; Prevalence of *ABCA12* Mutations as a Causative Gene for ARCI Patients

ARCI is a basket diagnosis, and HI, CIE, and LI are the major subtypes comprising the ARCI group. Among the 48 HI families in whom *ABCA12* mutation analysis has been reported (Supp. Table S1), ABCA12 mutations have been identified in all HI families; the *ABCA12* mutation detection rate is 100% (48/48) in the HI families. Kelsell et al. [2005] reported one HI patient in whom *ABCA12* mutation was not detected by direct sequencing analysis. However, multiplex PCR and oligonucleotide array analysis subsequently revealed deletion of exon 8 in this patient [Thomas et al., 2006]. In this context, HI is thought to be genetically homogeneous for causal *ABCA12* mutations.

In contrast, CIE and LI, the other two ARCI subtypes, to date, six genes, *ABCA12* [Lefèvre et al., 2003], *TGM1* [Huber et al., 1995; Russell et al., 1995], *ALOX12B* (MIM# 603741) [Jobard et al., 2002], *ALOXE3* (MIM# 607206) [Jobard et al., 2002], *ICHTHYIN* (MIM# 609383) [Lefèvre et al., 2004] and *FLJ39501* (MIM# 611495) [Lefèvre, 2006], have been reported to cause CIE; and four out of these six, *ABCA12* [Lefèvre et al., 2003], *TGM1* [Huber et al., 1995; Russell et al., 1995], *ALOX12B* [Jobard et al., 2002], and *ICHTHYIN* [Lefèvre et al., 2004], are also known to underlie LI. Recently, Fischer [2009] reported that in her cohort of 520 patients from 520 independent families with LI and CIE, causative mutations were detected by direct sequencing analysis in 78% of the patients. Only 5% of the patients were harbored *ABCA12* mutations although only exons 28–32 of *ABCA12* were sequenced for the majority of the patients in this study [Fischer, 2009]. The results suggest that ABCA12 is rather a minor cause for ARCI probably in the European and African populations, although the exact ethnic background of the 520 families was not provided in the report. Different from the situation in Europe, from the results of our mutation search, *ABCA12* mutations were frequently found in CIE families, but not in LI families, at least in the Japanese population [Sakai et al., 2009]. Thus, there might be a difference in the prevalence of causative genes for CIE and LI between the global subpopulations.

Genotype–Phenotype Correlation in *ABCA12* Mutations

Several genotype/phenotype correlations with *ABCA12* mutations have now come to light.

In HI (Supp. Fig. S1A), 44 *ABCA12* mutations were reported to date. Among them, most mutations are truncation mutations including nonsense mutations, frameshift mutations (deletion/insertion mutations), and splice site mutations (Table 1). Other mutations reported in HI families are missense mutations, exon deletions, and single amino acid deletions.

Most truncation or deletion mutations underlying HI are thought to lead to severe loss of ABCA12 protein function affecting important nucleotide-binding fold domains and/or transmembrane domains. Thus far, in HI patients, at least one mutation on each allele must be a truncation or deletion mutation

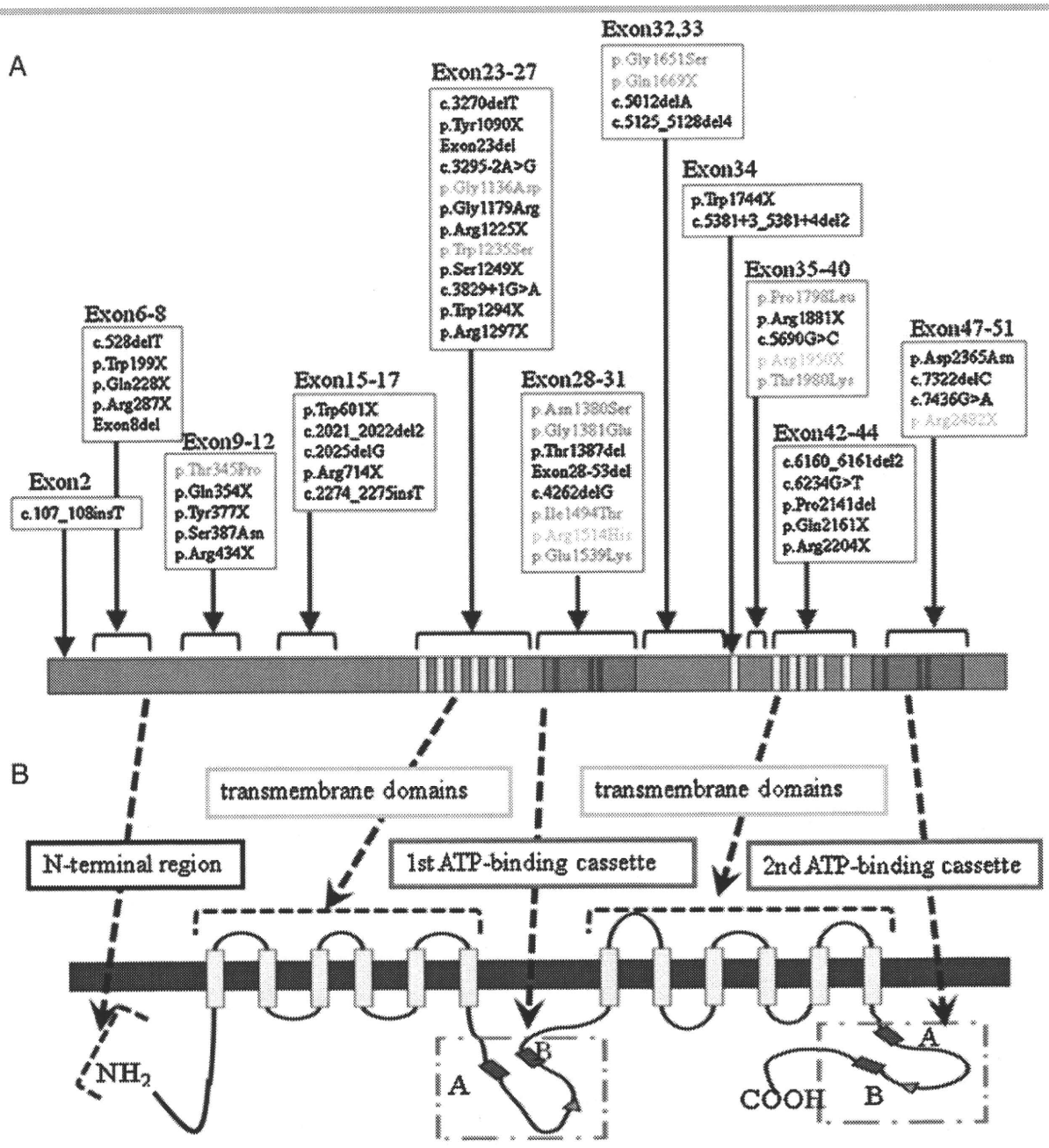

Figure 1. *ABCA12* mutations associated with autosomal recessive congenital ichthyosis. **A:** Reported *ABCA12* mutations and their localization within the *ABCA12* cDNA sequence. Mutations in black, red, and blue characters underlie HI, CIE, and LI, respectively. Mutations in green letters lead to two distinct phenotypes, p.Arg1950Ter and p.Arg2482Ter both result in CIE and HI phenotypes; p.Arg1514His underlies both CIE and LI phenotypes. Nucleotide numbering reflects cDNA numbering with +1 corresponding to the A of the ATG translation initiation codon in the reference sequence (GenBank NM_173076.2), according to journal guidelines (www.hgvs.org/mutnomen). The initiation codon is codon 1. **B:** ABCA12 protein structure and domains. Analysis of the ABCA12 predicted protein disclosed features that are typical of ABCA transporters, and the position of the conserved ATP-binding cassettes as well as that of the two transmembrane domains, each composed of six well-defined hydrophobic helices [Annilo et al., 2002]. See Supp. Table S1 for a complete list of mutations with both DNA and protein names.

within a conserved region to cause serious loss of ABCA12 function [Akiyama et al., 2005, 2006a,b, 2007a, b; Castiglia et al., 2009; Kelsell et al., 2005; Rajpar et al., 2006; Thomas et al., 2006, 2008]. Complete loss of ABCA12 function due to homozygous or compound heterozygous truncation mutations always results in the HI patient phenotype (Table 1).

In contrast, most mutations underlying LI and CIE are missense mutations and are expected to affect ABCA12 function more modestly.

In LI, five *ABCA12* mutations were reported in nine families and all the patients were homozygotes or compound heterozygotes for the mutations [Lefèvre et al., 2003]. None of the LI mutations was demonstrated to cause HI phenotype, although one mutation p.Arg1514His was identified to result in both LI and CIE phenotypes (Supp. Table S1). All the five mutations were missense mutations resulting in only one amino acid alteration in the first ATP-binding cassette of the ABCA12 peptide [Lefèvre et al., 2003] (Table 1). All the families were from Africa [Lefèvre

Table 1. Genotype/Phenotype Correlation in *ABCA12* Mutations in Harlequin Ichthyosis (HI), Congenital Ichthyosiform Erythroderma (CIE), and Lamellar Ichthyosis (LI)

Genotype →	Phenotype
[truncation] + [truncation]	HI
[truncation] + [exon or conserved amino acid deletion]	HI
[exon or conserved amino acid deletion] + [exon or conserved amino acid deletion]	HI
[truncation] + [missense]	HI, CIE
[exon or conserved amino acid deletion] + [missense mutation]	HI, CIE
[missense] + [missense]	LI, CIE
Phenotype →	**Genotype**
HI	[truncation] + [truncation]
	[truncation] + [exon or conserved amino acid deletion]
	[exon or conserved amino acid deletion] + [exon or conserved amino acid deletion]
	[truncation] + [missense mutation]
	[exon or conserved amino acid deletion] + [missense mutation]
LI	[missense] + [missense]
CIE	[missense] + [missense]
	[missense] + [truncation]
	[missense mutation] + [exon or conserved amino acid deletion]

et al., 2003]. These LI patients showed clinically generalized LI with large dark pigmented scales, ectropion, palmoplantar keratoderma and no erythema. They were born as collodion babies.

CIE patients (Supp. Fig. S1B) were also reported to harbor *ABCA12* mutations as the causative genetic defect [Akiyama et al., 2008; Natsuga et al., 2007; Sakai et al., 2009]. To date, 10 *ABCA12* mutations have been reported in eight CIE families. Two mutations, p.Arg1950Ter and p.Arg2482Ter, were identified to cause both CIE and HI disease phenotypes (Supp. Table S1). Only one mutation p.Arg1514His was reported to underlie both CIE and LI phenotypes (Supp. Table S1). In CIE, most underlying mutations are missense mutations. At least one mutation on each allele is a missense mutation in CIE (Table 1). In the CIE cases with *ABCA12* mutations, the scales are slightly larger than those in typical CIE cases and are classified as "medium sized" rather than "fine" scales.

Intrafamilial variation, for example, of CIE and HI cases from one family, has never as yet been reported. Thus, there is no evidence that any other gene(s) in these patients play a noticeable role affecting the phenotypes.

Further accumulation of patients and their *ABCA12* mutation data is needed to better elucidate genotype/phenotype correlations and will aid in predicting patients' prognosis.

Biological Significance; Pathomechanisms of Ichthyosis Involving *ABCA12* Mutations

In HI affected epidermis, several morphologic abnormalities including abnormal lamellar granules in the keratinocyte granular layer and a lack of extracellular lipid lamellae within the stratum corneum had been reported [Akiyama et al., 1994, 1998; Dale et al., 1990; Milner et al., 1992]. Lack of ABCA12 function subsequently leads to disruption of lamellar granule lipid transport in the upper keratinizing epidermal cells resulting in malformation of the intercellular lipid layers of the stratum corneum in HI [Akiyama et al., 2005] (Fig. 2). Cultured epidermal keratinocytes from an HI patient carrying *ABCA12* mutations demonstrated defective glucosylceramide transport, and this phenotype was recoverable by in vitro *ABCA12* corrective gene transfer [Akiyama et al., 2005]. To date, intracytoplasmic glucosylceramide transport has been studied using cultured keratinocytes from a total of three patients harboring *ABCA12* mutations. One patient was a homozygote for a splice site mutation c.3295−2A>G [Akiyama et al., 2005] and another patient was a compound heterozygote for p.Ser387Asn and p.Thr1387del [Akiyama et al., 2006a]. Only one heterozygous mutation p.Ile1494Thr was identified in the other patient [Natsuga et al., 2007]. Cultured keratinocytes from all the three patients showed apparently disturbed glucosylceramide transport, although this assay is not quantitative.

Interestingly, ABCA3, a member of the same protein superfamily as ABCA12, functions in pulmonary surfactant lipid secretion again via the production of similar lamellar-type granules within lung alveolar type II cells [Shulenin et al., 2004; Yamano et al., 2001].

In addition, defective lamellar granule formation was observed in the skin of two CIE patients with *ABCA12* mutations [Natsuga et al., 2007]. Electron microscopic observation revealed that, in the cytoplasm of granular layer keratinocytes, abnormal, defective lamellar granules were assembled together with some normal-appearing lamellar granules [Natsuga et al., 2007].

Formation of the intercellular lipid layers is essential for epidermal barrier function. In ichthyotic skin with ABCA12 deficiency, defective formation of the lipid layers is thought to result in a serious loss of barrier function and a likely extensive compensatory hyperkeratosis [Akiyama, 2006b].

A study in one *Abca12* disrupted *Abca12*$^{-/-}$ HI model mouse indicated that a lack of desquamation of skin cells, rather than enhanced proliferation of basal layer keratinocytes, accounts for the fivefold thickening of the *Abca12*$^{-/-}$ stratum corneum using in vivo skin proliferation measurements [Zuo et al., 2008]. It was suggested that this lack of desquamation was associated with a profound reduction in skin linoleic esters of long-chain ω-hydroxyceramides and a corresponding increase in their glucosylceramide precursors. ω-hydroxyceramides are required for correct skin barrier function, and these results from the HI model mice establish that ABCA12 activity is required for the generation of long-chain ceramide esters that are essential for the development of normal skin structure and function [Zuo et al., 2008].

One hypothetical pathomechanism for ABCA12 deficient in ARCI is the differentiation defect theory (Fig. 2), derived from the clinical features of HI patients. Fetuses affected with HI start developing their ichthyotic phenotype while they are in the

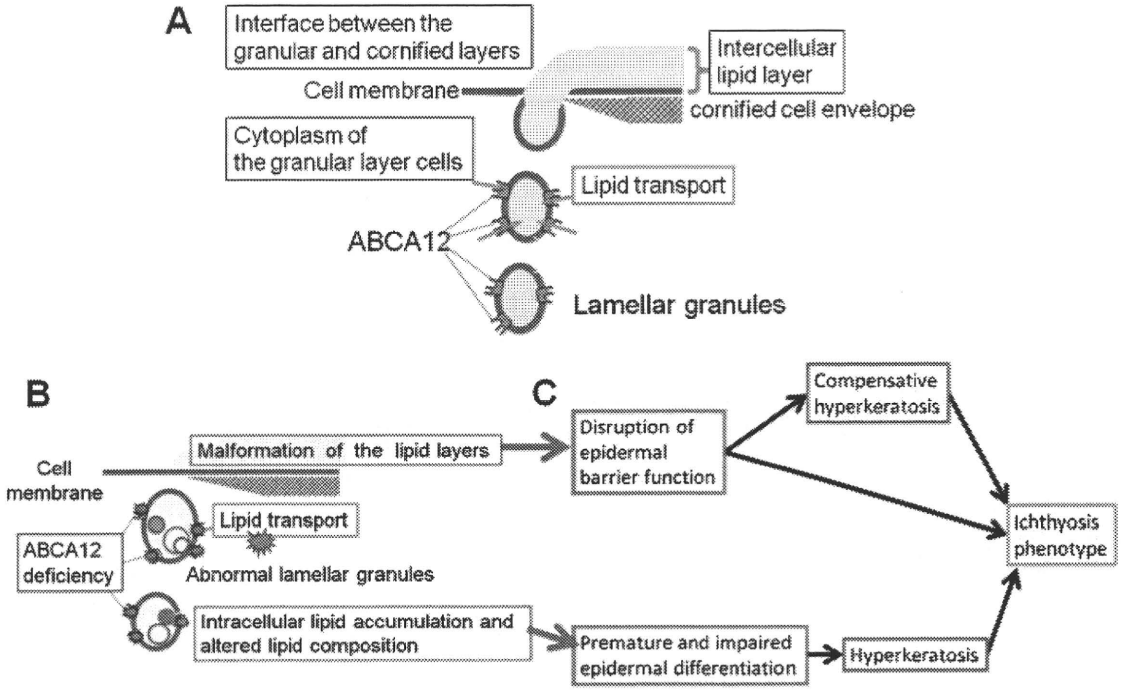

Figure 2. Physiological role(s) of ABCA12 in lipid trafficking of epidermal keratinocytes and the model of ichthyotic pathogenetic mechanisms underlying ABCA12 deficiency. **A:** Model of how ABCA12 transports lipids for keratinocyte differentiation and epidermal barrier function. ABCA12 in the limiting membrane of lamellar granules transports lipid into the lamellar granules. Accumulated lipid contents in the lamellar granules are secreted to the intercellular space forming the intercellular lipid layers, which are important for epidermal barrier function. **B:** Model of how loss of ABCA12 function leads to lipid abnormality and lipid barrier malformation in the upper epidermis. Loss-of-function mutations in ABCA12 disrupts lipid accumulation into the lamellar granules and normal lamellar granule formation, resulting in disturbed lipid transport and secretion to the extracellular space and abnormal lipid deposit in the cytoplasm. **C:** Disruption of epidermal barrier function and epidermal differentiation defects result from malformation of the stratum corneum lipid layers and abnormal intracellular lipid accumulation, respectively. It is hypothesized that lipid barrier defects and disturbed keratinocyte differentiation coordinately cause hyperkeratosis and the ichthyosis phenotype.

amniotic fluid where stratum corneum barrier function is not required. Thus, barrier defects cannot be involved directly in the pathogenesis of HI phenotype, at least during the in utero fetal period. In this context, disturbed keratinocyte differentiation is speculated to play an important role in the pathogenesis of HI phenotype. In fact, three dimensional culture studies revealed that HI keratinocytes differentiate poorly using morphologic criteria, and show reduced expression of keratin 1 and defective conversion from profilaggrin to filaggrin [Fleckman et al., 1997].

In an *ABCA12* ablated organotypic coculture system, an in vitro model of HI skin, expression of keratinocyte late differentiation-specific molecules was dysregulated [Thomas et al., 2009]. Expression of specific proteases associated with desquamation, kallikrein 5 and cathepsin D, was dramatically reduced in the ABCA12 ablated organotypic coculture system [Thomas et al., 2009]. In the model system, *ABCA12* ablation resulted in a premature terminal differentiation phenotype [Thomas et al., 2009]. Furthermore, in the mutant mice carrying a homozygous spontaneous missense mutation, loss of Abca12 function led to premature differentiation of basal keratinocytes [Smyth et al., 2008]. In contrast, in our *Abca12*$^{-/-}$ HI model mice, immunofluorescence and immunoblotting of *Abca12*$^{-/-}$ neonatal epidermis revealed defective profilaggrin/filaggrin conversion and reduced expression of the differentiation-specific molecules, loricrin, kallikrein 5, and transglutaminase 1, although their mRNA expression was upregulated [Yanagi et al., 2010]. These data suggest that ABCA12 deficiency may lead to disturbed keratinocyte differentiation during fetal development, resulting in an ichthyotic phenotype at birth. From these observations, ABCA12 deficiency might have global effects on keratinocyte differentiation, resulting in both impaired terminal differentiation and premature differentiation of the epidermis.

Animal Models

Recently, bioengineered disease models were established to investigate ichthyotic pathomechanisms due to ABCA12 defective function and to aid development of innovative treatments for ichthyosis with ABCA12 deficiency.

We transplanted cultured keratinocytes from patients with HI and succeeded in reconstituting HI skin lesions in immunodeficient mice [Yamanaka et al., 2007]. These reconstructed HI lesions showed similar changes to those observed in HI patients' skin. In addition, we generated *Abca12* disrupted (*Abca12*$^{-/-}$) mice and our *Abca12*$^{-/-}$ mice closely reproduced the human HI phenotype, showing marked hyperkeratosis with eclabium and skin fissure [Yanagi et al., 2008a]. Lamellar granule abnormalities and defective ceramide distribution were remarkable in the epidermis. Skin permeability assays of *Abca12*$^{-/-}$ mouse fetuses revealed severe skin barrier dysfunction after the initiation of keratinization. Surprisingly, *Abca12*$^{-/-}$ mice also demonstrated lung alveolar collapse immediately after birth. Lamellar bodies in alveolar type II cells from *Abca12*$^{-/-}$ mice lacked normal lamellar structures [Yanagi et al., 2008a]. The level of surfactant protein B, an essential component of alveolar surfactant, was reduced in the *Abca12*$^{-/-}$ mice [Yanagi et al., 2008a]. Another group independently

developed *Abca12*$^{-/-}$ mice and the mice also confirmed the clinical features of HI [Zuo et al., 2008]. In addition, a mouse strain carrying a homozygous spontaneous missense mutation was reported to show skin manifestations similar to ichthyosis [Smyth et al., 2008]. Lipid analysis in *Abca12* mutant epidermis revealed defects in lipid homeostasis, suggesting that *Abca12* plays a crucial role in maintaining lipid balance in the skin [Smyth et al., 2008]. The cells from the *Abca12* mutant mouse have severely impaired lipid efflux and intracellular accumulation of neutral lipids [Smyth et al., 2008]. Abca12 was also demonstrated as a mediator of Abca1-regulated cellular cholesterol efflux [Smyth et al., 2008]. Injection of a morpholino designed to target a splice site at the exon 4/intron 4 junction to block *Abca12* pre-mRNA processing induced altered skin surface contours, disorganization of the melanophore distribution, pericardial edema and enlargement of the yolk sac at 3 days postfertilization in the larvae of the zebrafish. It was also associated with premature death at around 6 days postfertilization. These results suggest that *Abca12* is an essential gene for normal zebrafish skin development and provide novel insight into the function of ABCA12 [reported at the Annual Meeting of the Society for Investigative Dermatology 2010; Abstract, Frank et al. J Invest Dermatol 2010;130:S86].

HI patients often die in the first 1 or 2 weeks of life. However, once they survive beyond the neonatal period, HI survivors' phenotypes improve within several weeks after birth. In order to clarify mechanisms of the phenotype recovery, we studied grafted skin and keratinocytes from *Abca12*-disrupted (*Abca12*$^{-/-}$) mouse [Yanagi et al., 2010]. *Abca12*$^{-/-}$ skin grafts kept in a dry environment exhibited dramatic improvements in all the abnormalities seen in the model mice. Increased transepidermal water loss, a parameter of barrier defect, was remarkably decreased in grafted *Abca12*$^{-/-}$ skin. 10 passage-subcultured *Abca12*$^{-/-}$ keratinocytes showed restoration of intact ceramide distribution, differentiation-specific protein expression, and profilaggrin/filaggrin conversion, which were defective in the primary culture [Yanagi et al., 2010]. These observations suggested that, during maturation, *Abca12*$^{-/-}$ epidermal keratinocytes regain normal differentiation processes, although the exact mechanisms of this restoration is still unknown [Yanagi et al., 2010].

We tried fetal therapy with systemic administration of retinoid or dexamethasone, which are effective treatments for neonatal HI and neonatal respiratory distress, respectively, to the pregnant mother mice; however, neither improved the skin phenotype or extended the survival period [Yanagi et al., 2008a]. Retinoids were also ineffective in in vivo studies using cultured keratinocytes from the model mice [Yanagi et al., 2010].

Prenatal Diagnosis of Harlequin Ichthyosis

In families with a history of HI, the parents' request for prenatal diagnosis is not easily ignored.

Before the causative gene for HI was identified, prenatal diagnosis had been performed by fetal skin biopsy and electron microscopic observation during the later stages of pregnancies at 19–23 weeks estimated gestational age for more than 20 years [Akiyama et al., 1994, 1999; Blanchet-Bardon et al., 1983; Shimizu et al., 2005]. The late timing of prenatal testing was a heavy burden on the pregnant mothers. In addition, when a fetus was diagnosed as affected, it was a major problem to induce a therapeutic termination at that late stage of pregnancy. After identification of *ABCA12* as the causative gene for HI, it has become feasible to perform DNA-based prenatal diagnosis for HI by chorionic villus or amniotic fluid sampling at a much earlier stage of pregnancy, with a significantly lower risk to fetal health and a reduced burden on mothers [Akiyama et al., 2007b]. Indeed, prenatal diagnosis and exclusion of HI by DNA testing were performed in our laboratory [Akiyama et al., 2007b; Yanagi et al., 2008b].

In the near future, it is hoped that much earlier prenatal diagnosis by completely noninvasive analysis of DNA from fetal cells in maternal circulation [Uitto et al., 2003] and preimplantation genetic diagnosis [Fassihi et al., 2006; Wells and Delhantry, 2001] will be available for HI.

Acknowledgments

I thank the ARCI families for their participation in this research. I also thank Dr. James R. McMillan for his proofreading and comments in the preparation of the manuscript, and Kaori Sakai, M.S., for her technical assistance. Grant sponsor: Grant-in-Aid from the Ministry of Education, Science, Sports, and Culture of Japan (to M. Akiyama); grant number: Kiban B 20390304. Grant sponsor: Ministry of Health, Labor and Welfare of Japan (Health and Labor Sciences Research Grants; Research on Intractable Disease; grant number: H22-Nanchi-Ippan-177 (to M. Akiyama). *ABCA12* mutation database is available at our site http://www.derm-hokudai.jp/ABCA12/.

References

Akiyama M. 2006a. Pathomechanisms of harlequin ichthyosis and ABCA transporters in human diseases. Arch Dermatol 142:914–918.

Akiyama M. 2006b. Harlequin ichthyosis and other autosomal recessive congenital ichthyoses: the underlying genetic defects and pathomechanisms. J Dermatol Sci 42:83–89.

Akiyama M, Dale BA, Smith LT, Shimizu H, Holbrook KA. 1998. Regional difference in expression of characteristic abnormality of harlequin ichthyosis in affected fetuses. Prenat Diagn 18:425–436.

Akiyama M, Kim D-K, Main DM, Otto CE, Holbrook KA. 1994. Characteristic morphologic abnormality of harlequin ichthyosis detected in amniotic fluid cells. J Invest Dermatol 102:210–213.

Akiyama M, Sakai K, Hatamochi A, Yamazaki S, McMillan JR, Shimizu H. 2008. Novel compound heterozygous nonsense and missense *ABCA12* mutations lead to non-bullous congenital ichthyosiform erythroderma. Br J Dermatol 158: 864–867.

Akiyama M, Sakai K, Sato T, McMillan JR, Goto M, Sawamura D, Shimizu H. 2007a. Compound heterozygous *ABCA12* mutations including a novel nonsense mutation underlie harlequin ichthyosis. Dermatology 215:155–159.

Akiyama M, Sakai K, Sugiyama-Nakagiri Y, Yamanaka Y, McMillan JR, Sawamura D, Niizeki H, Miyagawa S, Shimizu H. 2006a. Compound heterozygous mutations including a de novo missense mutation in ABCA12 led to a case of harlequin ichthyosis with moderate clinical severity. J Invest Dermatol 126:1518–1523.

Akiyama M, Sakai K, Wolff G, Hausser I, McMillan JR, Sawamura D, Shimizu H. 2006b. A novel ABCA12 mutation 3270delT causes harlequin ichthyosis. Br J Dermatol 155:1064–1066.

Akiyama M, Sawamura D, Shimizu H. 2003. The clinical spectrum of non-bullous congenital ichthyosiform erythroderma and lamellar ichthyosis. Clin Exp Dermatol 28:235–240.

Akiyama M, Shimizu H. 2008. An update on molecular aspects of the non-syndromic ichthyoses. Exp Dermatol 17:373–382.

Akiyama M, Sugiyama-Nakagiri Y, Sakai K, McMillan JR, Goto M, Arita K, Tsuji-Abe Y, Tabata N, Matsuoka K, Sasaki R, Sawamura D, Shimizu H. 2005. Mutations in ABCA12 in harlequin ichthyosis and functional rescue by corrective gene transfer. J Clin Invest 115:1777–1784.

Akiyama M, Suzumori K, Shimizu H. 1999. Prenatal diagnosis of harlequin ichthyosis by the examinations of keratinized hair canals and amniotic fluid cells at 19 weeks' estimated gestational age. Prenat Diagn 19:167–171.

Akiyama M, Titeux M, Sakai K, McMillan JR, Tonasso L, Calvas P, Jossic F, Hovnanian A, Shimizu H. 2007b. DNA-based prenatal diagnosis of harlequin ichthyosis and characterization of ABCA12 mutation consequences. J Invest Dermatol 127:568–573.

Annilo T, Shulenin S, Chen ZQ, Arnould I, Prades C, Lemoine C, Maintoux-Larois C, Devaud C, Dean M, Denèfle P, Rosier M. 2002. Identification and characterization of a novel ABCA subfamily member, ABCA12, located in the lamellar ichthyosis region on 2q34. Cytogenet Genome Res 98:169–176.

Blanchet-Bardon C, Dumez Y, Labbé F, Lutzner MA, Puissant A, Henrion R, Bernheim A. 1983. Prenatal diagnosis of harlequin fetus. Lancet I:132.

Borst P, Elferink RO. 2002. Mammalian ABC transporters in health and disease. Annu Rev Biochem 71:537–592.

Brash AR, Zheyong Y, Boeglin WE, Schneider C. 2007. The hepoxilin connection in the epidermis. FEBS J 274:3494–3502.

Castiglia D, Castori M, Pisaneschi E, Sommi M, Covaciu C, Zambruno G, Fischer J, Magnani C. 2009. Trisomic rescue causing reduction to homozygosity for a novel ABCA12 mutation in harlequin ichthyosis. Clin Genet 76:392–397.

Dale BA, Holbrook KA, Fleckman P, Kimball JR, Brumbaugh S, Sybert VP. 1990. Heterogeneity in harlequin ichthyosis, an inborn error of epidermal keratinization: variable morphology and structural protein expression and a defect in lamellar granules. J Invest Dermatol 94:6–18.

Fassihi H, Eady RAJ, Mellerio JE, Ashton GH, Dopping-Hepenstal PJ, Denyer JE, Nicolaides KH, Rodeck CH, McGrath JA. 2006. Prenatal diagnosis for severe inherited skin disorders: 25 years' experience. Br J Dermatol 154:106–113.

Fischer J. 2009. Autosomal recessive congenital ichthyosis. J Invest Dermatol 129: 1319–1321.

Fleckman P, Hager B, Dale BA. 1997. Harlequin ichthyosis keratinocytes in lifted culture differentiate poorly by morphologic and biochemical criteria. J Invest Dermatol 109:36–38.

Herman ML, Farasat S, Steinbach PJ, Wei M-H, Toure O, Fleckman P, Blake P, Bale SJ, Toro JR. 2009. Transglutaminase-1 gene mutations in autosomal recessive congenital ichthyosis: summary of mutations (including 23 novel) and modeling of TGase-1. Hum Mutat 30:537–547.

Huber M, Rettler I, Bernasconi K, Frenk E, Lavrijsen SP, Ponec M, Bon A, Lautenschlager S, Schorderet DF, Hohl D. 1995. Mutations of keratinocyte transglutaminase in lamellar ichthyosis. Science 267:525–528.

Jobard F, Lefèvre C, Karaduman A, Blanchet-Bardon C, Emre S, Weissenbach J, Ozgüc M, Lathrop M, Prud'homme JF, Fischer J. 2002. Lipoxygenase-3 (ALOXE3) and 12(R)-lipoxygenase (ALOX12B) are mutated in non-bullous congenital ichthyosiform erythroderma (NCIE) linked to chromosome 17p13.1. Hum Mol Genet 11:107–113.

Kelsell DP, Norgett EE, Unsworth H, Teh MT, Cullup T, Mein CA, Dopping-Hepenstal PJ, Dale BA, Tadini G, Fleckman P, Stephens KG, Sybert VP, Mallory SB, North BV, Witt DR, Sprecher E, Taylor AE, Ilchyshyn A, Kennedy CT, Goodyear H, Moss C, Paige D, Harper JI, Young BD, Leigh IM, Eady RA, O'Toole EA. 2005. Mutations in *ABCA12* underlie the severe congenital skin disease harlequin ichthyosis. Am J Hum Genet 76:794–803.

Lefèvre C, Audebert S, Jobard F, Bouadjar B, Lakhdar H, Boughdene-Stambouli O, Blanchet-Bardon C, Heilig R, Foglio M, Weissenbach J, Lathrop M, Prud'homme JF, Fischer J. 2003. Mutations in the transporter ABCA12 are associated with lamellar ichthyosis type 2. Hum Mol Genet 12:2369–2378.

Lefèvre 2006. Mutations in a new cytochrome P450 gene in lamellar ichthyosis type 3. Hum Mol Genet 15:767–776.

Lefèvre C, Bouadjar B, Karaduman A, Jobard F, Saker S, Ozguc M, Lathrop M, Prud'homme JF, Fischer J. 2004. Mutations in ichthyin a new gene on chromosome 5q33 in a new form of autosomal recessive congenital ichthyosis. Hum Mol Genet 13:2473–2482.

Milner ME, O'Guin WM, Holbrook KA, Dale BA. 1992. Abnormal lamellar granules in harlequin ichthyosis. J Invest Dermatol 99:824–829.

Natsuga K, Akiyama M, Kato N, Sakai K, Sugiyama-Nakagiri Y, Nishimura M, Hata H, Abe M, Arita K, Tsuji-Abe Y, Onozuka T, Aoyagi S, Kodama K, Ujiie H, Tomita Y, Shimizu H. 2007. Novel ABCA12 mutations identified in two cases of non-bullous congenital ichthyosiform erythroderma associated with multiple skin malignant neoplasia. J Invest Dermatol 127:2669–2673.

Peelman F, Labeur C, Vanloo B, Roosbeek S, Devaud C, Duverger N, Denèfle P, Rosier M, Vandekerckhove J, Rosseneu M. 2003. Characterization of the ABCA transporter subfamily: identification of prokaryotic and eukaryotic members, phylogeny and topology. J Mol Biol 325:259–274.

Rajpar SF, Cullup T, Kelsell DP, Moss C. 2006. A novel ABCA12 mutation underlying a case of harlequin ichthyosis. Br J Dermatol 155:204–206.

Russell LJ, DiGiovanna JJ, Rogers GR, Steinert PM, Hashem N, Compton JG, Bale SJ. 1995. Mutations in the gene for transglutaminase 1 in autosomal recessive lamellar ichthyosis. Nat Genet 9:279–283.

Sakai K, Akiyama M, Sugiyama-Nakagiri Y, McMillan JR, Sawamura D, Shimizu H. 2007. Localization of ABCA12 from Golgi apparatus to lamellar granules in human upper epidermal keratinocytes. Exp Dermatol 16:920–926.

Sakai K, Akiyama M, Yanagi T, McMillan JR, Suzuki T, Tsukamoto K, Sugiyama H, Hatano Y, Hayashitani M, Takamori K, Nakashima K, Shimizu H. 2009. ABCA12 is a major causative gene for non-bullous congenital ichthyosiform erythroderma. J Invest Dermatol 129:2306–2309.

Shimizu A, Akiyama M, Ishiko A, Yoshiike T, Suzumori K, Shimizu H. 2005. Prenatal exclusion of harlequin ichthyosis; potential pitfalls in the timing of the fetal skin biopsy. Br J Dermatol 153:811–814.

Shulenin S, Nogee LM, Annilo T, Wert SE, Whitsett JA, Dean M. 2004. ABCA3 gene mutations in newborns with fatal surfactant deficiency. N Engl J Med 350: 1296–1303.

Smyth I, Hacking DF, Hilton AA, Mukhamedova N, Meikle PJ, Ellis S, Slattery K, Collinge JE, de Graaf CA, Bahlo M, Sviridov D, Kile BT, Hilton DJ. 2008. A mouse model of harlequin ichthyosis delineates a key role for Abca12 in lipid homeostasis. PLoS Genet 4:e1000192.

Thomas AC, Cullup T, Norgett EE, Hill T, Barton S, Dale BA, Sprecher E, Sheridan E, Taylor AE, Wilroy RS, DeLozier C, Burrows N, Goodyear H, Fleckman P, Stephens KG, Mehta L, Watson RM, Graham R, Wolf R, Slavotinek A, Martin M, Bourn D, Mein CA, O'Toole EA, Kelsell DP. 2006. ABCA12 is the major harlequin ichthyosis gene. J Invest Dermatol 126:2408–2413.

Thomas AC, Sinclair C, Mahmud N, Cullup T, Mellerio JE, Harper J, Dale BA, Turc-Carel C, Hohl D, McGrath JA, Vahlquist A, Hellstrom-Pigg M, Ganemo A, Metcalfe K, Mein CA, O'Toole EA, Kelsell DP. 2008. Novel and recurring ABCA12 mutations associated with harlequin ichthyosis: implications for prenatal diagnosis. Br J Dermatol 158:611–613.

Thomas AC, Tattersall D, Norgett EE, O'Toole EA, Kelsell DP. 2009. Premature terminal differentiation and a reduction in specific proteases associated with loss of ABCA12 in harlequin ichthyosis. Am J Pathol 174:970–978.

Uitto J, Pfendner E, Jackson LG. 2003. Probing the fetal genome: progress in non-invasive prenatal diagnosis. Trends Mol Med 9:339–343.

Wells D, Delhantry JDA. 2001. Preimplantation genetic diagnosis: Applications of molecular medicine. Trends Mol Med 7:23–30.

Yamanaka Y, Akiyama M, Sugiyama-Nakagiri Y, Sakai K, Goto M, McMillan JR, Ota M, Sawamura D, Shimizu H. 2007. Expression of the keratinocyte lipid transporter ABCA12 in developing and reconstituted human epidermis. Am J Pathol 171:43–52.

Yamano G, Funahashi H, Kawanami O, Zhao LX, Ban N, Uchida Y, Morohoshi T, Ogawa J, Shioda S, Inagaki N. 2001. ABCA3 is a lamellar body membrane protein in human lung alveolar type II cells. FEBS Lett 508:221–225.

Yanagi T, Akiyama M, Nishihara H, Ishikawa J, Sakai K, Miyamura Y, Naoe A, Kitahara T, Tanaka S, Shimizu H. 2010. Self-improvement of keratinocyte differentiation defects during skin maturation in ABCA12 deficient harlequin ichthyosis model mice. Am J Pathol 177:106–118.

Yanagi T, Akiyama M, Nishihara H, Sakai K, Nishie W, Tanaka S, Shimizu H. 2008a. Harlequin ichthyosis model mouse reveals alveolar collapse and severe fetal skin barrier defects. Hum Mol Genet 17:3075–3083.

Yanagi T, Akiyama M, Sakai K, Nagasaki A, Ozawa N, Kosaki R, Sago H, Shimizu H. 2008b. DNA-based prenatal exclusion of harlequin ichthyosis. J Am Acad Dermatol 58:653–656.

Zuo Y, Zhuang DZ, Han R, Isaac G, Tobin JJ, McKee M, Welti R, Brissette JL, Fitzgerald ML, Freeman MW. 2008. ABCA12 maintains the epidermal lipid permeability barrier by facilitating formation of ceramide linoleic esters. J Biol Chem 283:36624–36635.

The American Journal of Pathology, Vol. 176, No. 4, April 2010

DOI: 10.2353/ajpath.2010.090597

Short Communication

Transglutaminase1 Preferred Substrate Peptide K5 Is an Efficient Tool in Diagnosis of Lamellar Ichthyosis

Masashi Akiyama,* Kaori Sakai,* Teruki Yanagi,* Satoshi Fukushima,† Hironobu Ihn,† Kiyotaka Hitomi,‡ and Hiroshi Shimizu*

From the Department of Dermatology, Hokkaido University Graduate School of Medicine, Sapporo; the Department of Dermatology and Plastic Surgery,† Graduate School of Medical and Pharmaceutical Sciences, Kumamoto University, Kumamoto; and the Department of Applied Molecular Biosciences,‡ Graduate School of Bioagricultural Sciences, Nagoya University, Japan*

Lamellar ichthyosis (LI) is a genetically heterogeneous, severe genodermatosis showing widespread hyperkeratosis of the skin. Transglutaminase 1 (TGase1) deficiency by TGase1 gene (*TGM1*) mutations is the most prevalent cause of LI. Screening of TGase1 deficiency in skin is essential to facilitate the molecular diagnosis of LI. However, cadaverine, the most widely used substrate for TGase activity assay, is not isozyme specific. Recently, a human TGase1–specific highly preferred substrate peptide K5 (pepK5) was generated. To evaluate its potential as a diagnostic tool for LI, we performed pepK5 labeling of TGase1 activity in normal human and LI skin. Ca^{2+}-dependent labeling of FITC-pepK5 was clearly seen in the upper spinous and granular layers of normal human skin where it precisely overlapped with TGase1 immunostaining. Both specificity and sensitivity of FITC-pepK5 labeling for TGase1 activity were higher than those of FITC-cadaverine labeling. FITC-pepK5 labeling colocalized with involucrin and loricrin immunostaining at cornified cell envelope forming sites. FITC-pepK5 labeling was negative in LI patients carrying *TGM1* truncation mutations and partially abolished in the other LI patients harboring missense mutations. The present results clearly indicate that pepK5 is a powerful tool for screening LI patient TGase1 deficiency when we make molecular diagnosis of LI. *(Am J Pathol 2010, 176:1592–1599; DOI: 10.2353/ajpath.2010.090597)*

One of the essential events during terminal differentiation of epidermal keratinocytes and skin barrier formation is the production of a 15-nm-thick layer of protein on the inner surface of the keratinocyte cell membrane, termed the cornified cell envelope (CCE). The CCE is assembled by the accumulation of several precursor proteins including involucrin and loricrin.[1] It is known that the precursor proteins are cross-linked together by the formation of N^{ε}-(γ-glutamyl) lysine isodipeptide bonds catalyzed by the action of transglutaminase isoforms. Transglutaminase 1 (TGase1) is a key enzyme in CCE formation in the epidermis.

Lamellar ichthyosis (LI) is a major subtype of autosomal recessive congenital ichthyosis and clinically characterized by large, thick, dark scales over the entire body without serious background erythroderma.[2] Since the identification of TGase1 gene (*TGM1*) mutations in a number of families with LI in 1995,[3,4] more than one hundred *TGM1* mutations have been reported in LI families. TGase1 deficiency attributable to *TGM1* mutations is a major underlying causative factor in LI patients,[5,6] although LI is thought to be a genetically heterogeneous disorder and several causative molecules including TGase1 have been identified.[3,4,7,8–11] Although genotype/phenotype correlations in autosomal recessive congenital ichthyosis including LI with *TGM1* mutations have been studied for years, the exact nature of the relationship has yet to be fully elucidated.[5,6,12–15] Thus, it is difficult to know whether a causative gene is *TGM1* or not in each LI patient from each patient's clinical features alone.

Supported in part by a grant from the Ministry of Education, Science, and Culture of Japan to M.A. (Kiban B 20390304) and by a grant from Ministry of Health, Labor, and Welfare of Japan (Health and Labor Sciences Research grants; Research on intractable diseases; H21-047) to M.A.

Accepted for publication November 23, 2009.

Address reprint requests to Masashi Akiyama, M.D., Ph.D., Department of Dermatology, Hokkaido University Graduate School of Medicine, North 15 West 7, Kita-ku, Sapporo 060-8638, Japan. E-mail: akiyama@med.hokudai.ac.jp.

To date, to facilitate molecular diagnosis in LI patients with *TGM1* mutations, *in situ* transglutaminase (TGase) activity assays have been performed using cadaverine as a substrate to detect TGase1 activity in the patients' skin,[16–20] despite the fact that cadaverine is not an isozyme-specific probe, and detects total TGase activity in the epidermis. Recently, a human TGase1 specific, highly preferred substrate peptide K5 (pepK5) was generated.[21] We hypothesized that, as previously shown in mouse skin, pepK5 would detect *in situ* TGase1 activity with high specificity and sensitivity in the human epidermis. If it is the case, pepK5 can be a useful tool to detect TGase1 deficiency in LI patients with *TGM1* mutations.

In the present study, we demonstrated that pepK5 can be used as an efficient probe to detect TGase1 activity in the human epidermis. In addition, we performed *in situ* TGase1 activity assay using pepK5 in skin specimens from LI patients with *TGM1* mutations and clearly revealed that this preferred substrate for TGase1, pepK5 is a powerful tool for evaluation of TGase1 activity in LI patients and for molecular diagnosis of LI.

Materials and Methods

Synthesis of Transglutaminase Substrate Peptides

PepK5, peptide K5QN (pepK5QN), and peptide form T26 (pepT26) were synthesized as previously described.[21,22] Briefly, a phage-displayed random peptide library was used to screen primary amino acid sequences that are preferentially selected by human TGase1. The peptides selected as glutamine donor substrate exhibited a marked tendency in primary structure, conforming to the sequence: QxK/RψxxxWP (where x and ψ represent nonconserved and hydrophobic amino acids, respectively). Using glutathione S-transferase (GST) fusion proteins of the selected peptides, several sequences were identified as preferred substrates and confirmed that they were isozyme-specific. The 12-aa peptide pepK5 (YEQHKLPSSWPF) was synthesized. Even in peptide form, K5 appeared to have high and specific reactivity as substrate. In addition, a mutant peptide in which glutamine was substituted by asparagine was also synthesized as pepK5QN (YENHKLPSSWPF). pepT26 (HQSYVDPWMLDH) was synthesized as the transglutaminase 2 (TGase2) preferred substrate peptide for comparison.[22] Finally, these synthesized peptides were conjugated with FITC.[21]

In Situ *TGase1 Activity Assay*

Skin sections were prepared from skin biopsy patient specimens and normal control specimens using standard methods.[21,23] The frozen sections were dissected into 6-μm slices and stored frozen at −80°C until use.

Sections were dried and then blocked with 1% BSA in NaCl/Pi at room temperature. The sections were incubated for 90 minutes with a solution containing 100 mmol/L Tris/HCl pH 8.0, 5 mmol/L $CaCl_2$ or 1 mmol/L EDTA, and 1 mmol/L dithiothreitol, in the presence of 5 μmol/L (or other concentrations) of FITC-labeled substrate peptide or FITC-cadaverine (Sigma-Aldrich, St. Louis, MO). This *in situ* TGase1 activity assay works by measuring the fluorescence of fluorescein isothiocyanate (FITC)-labeled substrate peptide incorporated into cellular proteins by cross-linking catalyzed by TGase1. After washing with NaCl/Pi three times for 5 minutes, antifading solution was added to the sections, which were then sealed with a cover glass and mountant. In addition, we performed the above-mentioned pepK5 labeling using normal human skin specimens and LI patients' skin samples under various incubation conditions (pH 7.4, 8.0 and 8.4; temperature 25°C, 33°C and 37°C).

Double Labeling for in Situ *TGase1 Assay and Immunofluorescence Staining*

For double labeling (*in situ* TGase1 activity assay and immunofluorescence), at first, we performed *in situ* TGase1 activity assay as described above, then the sections were labeled with immunofluorescence methods below. Immunofluorescence labeling was performed as described previously.[23] Primary antibodies used in this study were as follows: mouse monoclonal anti-TGase 1 antibody (B.C1; Biomedical Technologies, Inc., Stoughton, MA), rabbit polyclonal anti-TGase1 antibody (Novus Biologicals, LLC, Littleton, CO), anti-loricrin antibody (Covance Lab., Richmond, CA), and anti-involucrin antibody (Biomedical Technologies, Inc., Stoughton, MA). We used FITC-conjugated or tetramethylrhodamine-isothiocyanate (TRITC)-conjugated rabbit anti-mouse immunoglobulin (Jackson ImmunoResearch Laboratories, Inc. West Grove, PA) or donkey anti-rabbit immunoglobulins (DAKO, Glostrup, Denmark), as secondary antibodies.

Ichthyosis Patients Involved in the Present Study

In total, four unrelated LI patients with *TGM1* mutations were included in this study. Patient 1 was a recently examined LI case and the other three patients were reported previously.[6,20,24] As controls, two *TGM1*-unrelated autosomal recessive congenital ichthyosis patients harboring ABCA12 mutations[25] were also included in the present study.

Fully informed consent was obtained from the participants or their legal guardians for this study. This study had been previously evaluated and approved by the ethics committee at Hokkaido University Graduate School of Medicine and was conducted according to the Declaration of Helsinki Principles.

Mutation Search

TGM1 mutation search was performed as previously reported.[19] Briefly, genomic DNA isolated from peripheral blood was subjected to polymerase chain reaction amplification, followed by direct automated sequencing and verification of the mutation by restriction enzyme diges-

tions. Most oligonucleotide primers used for amplification of all 15 exons of *TGM1* have been reported elsewhere[12] and partially modified for the present study.[19] The entire coding regions of *TGM1* including the exon/intron boundaries were sequenced using genomic DNA samples from patients and their family members. One hundred normal alleles (50 unrelated, healthy Japanese individuals) were sequenced as normal controls.

Results

In Situ *Assay Using pepK5 Detected TGase1 Activity with High Specificity and Sensitivity in the Upper Epidermis of Normal Human Skin*

With the presence of $CaCl_2$ in the reaction mixture, we detected specific incorporation of FITC-labeled pepK5 (FITC-pepK5; 5 μmol/L) into substrate proteins in the epidermis, mainly at the cell periphery of the upper spinous and granular layers of normal human skin (Figure 1A). No signal was detected in the presence of EDTA (Figure 1B), or when we used FITC-conjugated pepK5QN mutant peptide (FITC-pepK5QN; Figure 1C), which indicated that the cross-linking reaction was catalyzed specifically by TGase1. Using FITC-conjugated pepT26 (FITC-pepT26), a preferable substrate for TGase2, only faint labeling was obtained around the granular layer cells and this labeling was abolished in the presence of EDTA (data not shown). Under various incubation conditions, pH 7.4, 8.0, and 8.4, temperature 25°C, 33°C, and 37°C, no significant difference in the pepK5 labeling intensity was observed in normal human epidermis (data not shown).

The FITC-pepK5 labeling pattern corresponded well with the localization of TGase1 by immunostaining with anti-TGase1 antibody. Double labeling for *in situ* TGase1 activity assay using FITC-pepK5 and immunostaining for TGase1 molecule showed completely overlapping colocalization of these moieties at the cell periphery of both the upper spinous and granular layer cells (Figure 1, D–F).

Double Labeling for TGase1 Activity with pepK5 and CCE Precursor Proteins Demonstrated that pepK5 Labeling Precisely Localized to Sites of CCE Formation

Immunofluorescence labeling for involucrin, a major CCE precursor protein, was seen in the upper half of the epidermis (Figure 1H). Double labeling for *in situ* TGase1 activity assay using pepK5, and involucrin immunolabeling showed that, in the upper spinous and granular cell layers, pepK5 labeling and involucrin co-localized at the cell periphery (Figure 1, G–I). In addition, double labeling for the *in situ* TGase1 activity assay using pepK5, and immunolabeling for loricrin, another major CCE precursor protein, revealed almost complete colocalization of

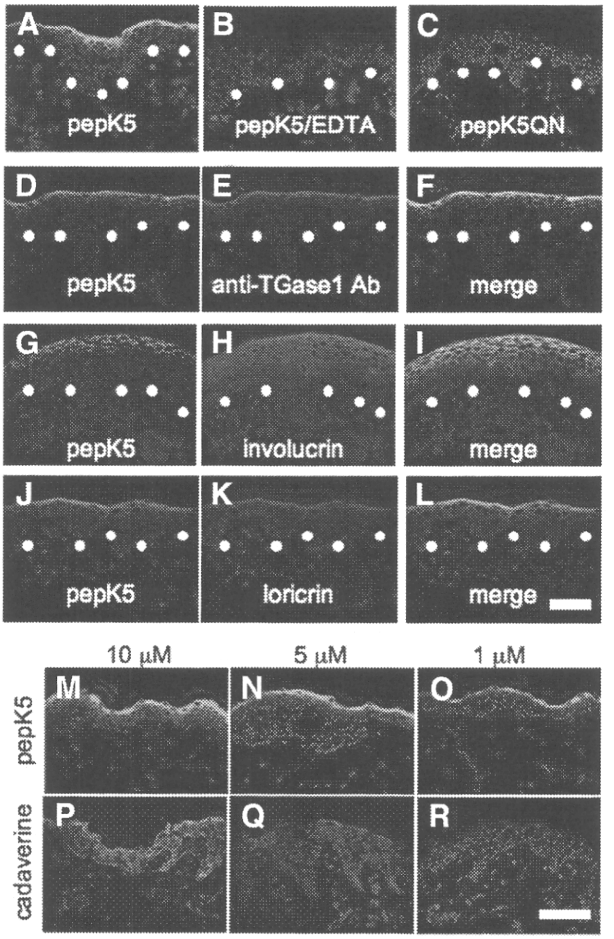

Figure 1. PepK5 labeling detected *in situ* TGase1 activity with high specificity and sensitivity at CCE forming sites in normal human skin. **A–C:** *In situ* TGase1 activity detected by pepK5 in normal skin. Detection of *in situ* TGase 1 activity using FITC-labeled pepK5 (5 μmol/L) showed intense membrane-restricted staining within the upper spinous and granular layer keratinocytes of a normal human skin (**A**). In the presence of EDTA, the pepK5 labeling was completely abolished (**B**). No labeling was observed with FITC-labeled mutant K5 peptide (pepK5QN; **C**). Specific labeling, green (FITC); nuclear stain, red (propidium iodide). **White dots**, basement membrane zone. **D–F:** Double labeling with pepK5 and anti-TGase1 antibody in normal human skin. Both pepK5 labeling (**D**, green, FITC) and anti-TGase1 antibody (B.C1) labeling (**E**, red, TRITC) are seen in the upper epidermis, mainly in the granular layers. The merged image clearly demonstrates that both labeling patterns almost completely overlap (yellow) each other on the cell membrane of the upper epidermal keratinocytes (**F**). pepK5 labeling, green (FITC), anti-TGase1 antibody labeling, red (TRITC); nuclear stain, blue (TOPRO). White dots, basement membrane zone. **G–L:** Double labeling with anti-CCE precursor protein antibodies and pepK5 in normal human skin. Anti-involucrin antibody labeling (**H**, red, TRITC) is seen in the upper half of the epidermis, although pepK5 labeling (**G**, green, FITC) is observed mainly in the uppermost spinous and granular cell layers. Involucrin and pepK5 labeling overlap each other (yellow) on the cell membrane of the uppermost spinous and granular cell layer keratinocytes in the merged image (**I**). Both pepK5 labeling (**J**, green, FITC) and anti-loricrin antibody labeling (**K**, red, TRITC) are seen mostly within the uppermost spinous and granular layers. The merged image shows that loricrin and pepK5 labeling clearly overlap (yellow) each other on the cell membrane of the granular layer keratinocytes (**L**). FITC-pepK5 labeling, green; anti-involucrin and anti-loricirn antibodies, red (TRITC); nuclear stain, blue (TOPRO). **White dots**, basement membrane zone. **M–R:** Detection of TGase1 activity in normal human skin sections using graded concentrations of pepK5 or cadaverine. Intense labeling is seen in the upper epidermis with 10 μmol/L (**M**) and 5 μmol/L (**N**) of FITC-pepK5. Only the granular layer keratinocytes are labeled with 1 μmol/L (**O**) of FITC-pepK5. Using 10 μmol/L (**P**) of FITC-cadaverine, all epidermal keratinocytes are labeled. With 5 μmol/L (**Q**) of FITC-cadaverine, entire epidermis is faintly labeled. No labeling is observed with 1 μmol/L (**R**) of FITC-cadaverine. **M–O:** FITC-pepK5 labeling, green; **P–R:** FITC-cadaverine labeling, green; nuclear stain, red (propidium iodide). Substrate concentrations, 10 μmol/L (**M**, **P**), 5 μmol/L (**N**, **Q**), 1 μmol/L (**O**, **R**). Scale bars = 50 μm.

A LI patients with *TGM1* mutations included in the present study

Patient No.	Age	Sex	*TGM1* mutations	Phenotype	Skin hyperkeratosis		References
					severity	localization	
1	0	M	p.[Arg106X]+[Gln234X]	LI (severe)	severe	generalized	this study
2	33	F	c.[371delA]+[=]	LI (severe)	severe	generalized	Ref. No. 24
3	0	M	p.[Arg307Trp]+[=]	LI (mild)	mild	localized (trunk)	Ref. No. 6
4	56	F	p.[Leu205Gln]+[Arg307Trp]	LI (mild)	mild	localized (trunk)	Ref. No. 20

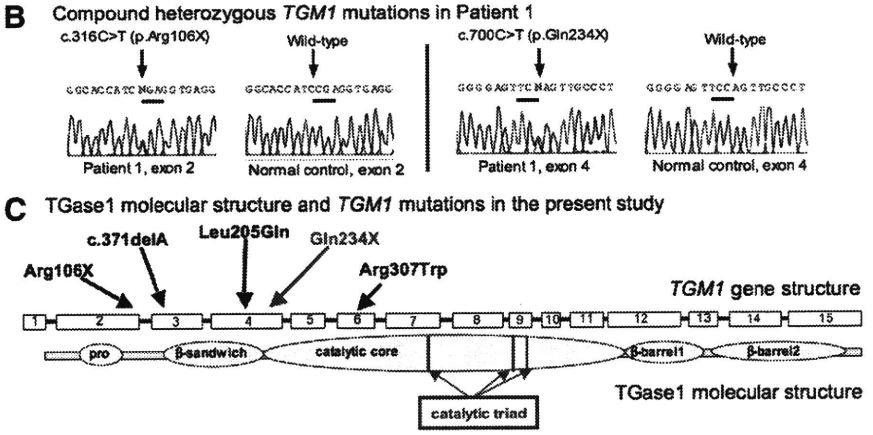

Figure 2. *TGM1* mutations and clinical features of LI patients in the present study. **A:** Summary of the *TGM1* mutations and phenotypes of the LI patients included in the present study. Note Patients 1 and 2 harbored truncation mutations in both alleles and exhibited a severe phenotype, and Patients 3 and 4 carried missense mutations in both alleles exhibiting a milder phenotype. An underlined mutation was a novel mutation. **B:** Direct sequence analysis of exons 2 and 4 of Patient 1 revealed heterozygous nonsense mutations, c.316C>T (p.Arg106X) and c.700C>T (p.Gln234X). **C:** Schematic sequential arrangement of the domain structure of the TGase1 polypeptide. Mutations in the present LI patients are marked by **arrows**. Red characters and **arrows** indicate novel mutations and black ones are previously reported mutations. Note that three truncation mutations are located upstream to the catalytic core domain. Two missense mutations are in the β-sandwich domain and the catalytic core domain, which are important for enzyme activity.

TGase1 activity and loricrin in the cell periphery of the upper spinous and granular layer cells (Figure 1, J–L).

PepK5 Detected in Situ *TGase1 Activity Efficiently Compared with Cadaverine*

We also compared the reactivity of FITC-pepK5 and FITC-cadaverine, which has been previously used for detection of *in situ* TGase activity in normal human skin at various concentrations, 10, 5, 1, and 0.1 μmol/L (Figure 1, M–R). At 10 μmol/L and 5 μmol/L concentrations, intense FITC-pepK5 labeling was observed mainly in the cell periphery of the upper spinous and granular layer keratinocytes in the normal human epidermis. At 1 μmol/L concentration, FITC-pepK5 labeled only the granular layer keratinocytes, and at 0.1 μmol/L concentration (data not shown) no FITC-pepK5 labeling was seen in the normal human epidermis. In contrast, using FITC-cadaverine at 10 μmol/L concentration, the entire epidermis was labeled, and at 5 μmol/L concentration only faint FITC-cadaverine labeling was seen in all of the layers of normal human epidermis. At 1 μmol/L or 0.1 μmol/L (data not shown) concentration, no FITC-cadaverine labeling was obtained in the epidermis. These results suggest that FITC-pepK5 detects endogenous TGase1 activity with greater sensitivity, at least more than ten times higher than FITC-cadaverine in human epidermis. In addition, considering the labeling patterns in the epidermis by the two substrates, specificity of pepK5 to TGase1 seemed to be much higher than that of cadaverine.

TGM1 Mutations and Clinical Features of LI Patients Involved in the Present Study

TGM1 mutations and clinical features of the patients included in the present study are summarized in Figure 2, A–C. Patients 1 and 2 showed a typical, classic LI phenotype. Patients 3 and 4 had a mild LI phenotype with mild hyperkeratosis mainly on the trunk. Patient 4 had a LI phenotype termed as "bathing suit ichthyosis"[26] with restricted affected regions on the trunk.

Patient 1 was a newly examined LI case. Patient 1 was compound heterozygous for the two *TGM1* nonsense mutations, p.Arg106X and p.Gln234X (c.[316C>T]+[700C>T]; p.[Arg106X]+[Gln234X]; Figure 2B) and showed a typical classic form of LI. One mutation p.Gln234X was a novel mutation and the other mutation p.Arg106X was previously reported.[27] These mutations were not found in 100 normal control alleles (50 unrelated, healthy Japanese individuals) and were not thought to be polymorphisms. The three other patients included in the present study had been reported previously to have a total of three *TGM1* mutations including p.Arg307Trp, a prevalent TGM1 mutation in the Japanese population.[6,20,24]

PepK5 Labeling Clearly Detected Defective TGase1 Activity in the Skin of LI Patients

In Patients 1 and 2, membranous TGase 1 activity detected by FITC-pepK5 in the upper spinous and granular layers of the patients' epidermis was completely lost (Figure 3, A and B). In Patient 3, membranous TGase 1 activity detected by FITC-pepK5 in the upper spinous and granular layers of the patient's epidermis was observed, but remarkably weaker (Figure 3C) than that of normal control human epidermis (Figure 3E). In Patient 4, membranous TGase1 activity demonstrated by FITC-pepK5 in the upper spinous and granular layers of the patient's epidermis was present, but restricted solely to the granular layer cells and cells just below the granular layer and was significantly weaker (Figure 3D) than that of normal control human epidermis (Figure 3E). In the

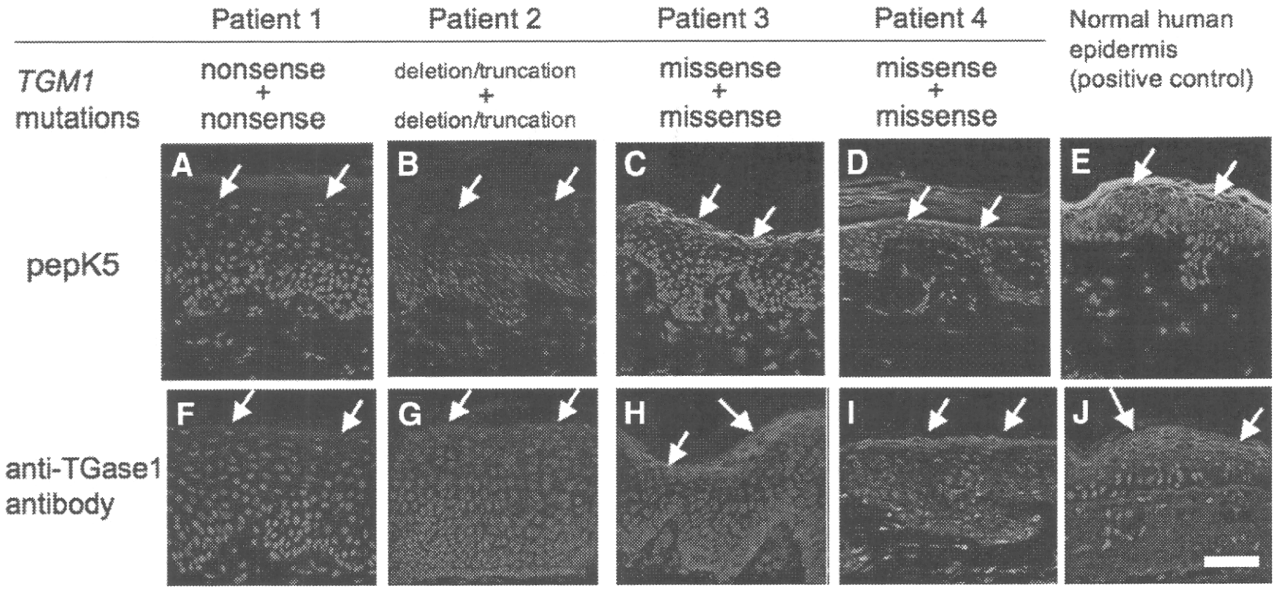

Figure 3. TGase1 deficiency detected by pepK5 labeling in the LI patients. **A and F:** Patient 1, a compound heterozygote for two *TGM1* nonsense mutations: FITC-pepK5 labeling (green) shows complete absence of TGase1 activity in the upper epidermis (**arrows**; **A**), and TGase1 immunostaining (green) is also negative in the upper epidermis (**arrows**; **F**). **B and G:** Patient 2, a homozygote for a *TGM1* deletion mutation causing truncation of the peptide: FITC-pepK5 labeling (green) reveals completely abolished TGase1 activity in the upper epidermis (**arrows**; **B**) and no TGase1 immunolabeling (in green) is seen in the upper epidermis (**arrows**; **G**). **C** and **H:** Patient 3, a homozygote for a *TGM1* missense mutation: detectable, but reduced membranous TGase1 activity is seen in the upper epidermis (**arrows**) by FITC-pepK5 labeling (green; **C**). TGase1 immunostaining (green) in the upper epidermis (**arrows**) confirms expression of TGase1 molecule (**H**). **D** and **I:** Patient 4, a compound heterozygote for two *TGM1* missense mutations: FITC-pepK5 labeling (green) shows faint TGase1 activity restricted to the granular layers (**arrows**; **D**). Immunofluorescence labeling for TGase1 (green) reveals a positive staining in the granular layer (**arrows**) in the patient's epidermis (**I**). **E and J:** In a normal human skin without any *TGM1* mutations, intense TGase1 activity is seen in the upper epidermis (**arrows**) using FITC-pepK5 labeling (green; **E**). TGase1 immunolabeling (green) is also positive in the upper epidermis (**arrows**; **J**). **A–E:** FITC-pepK5 labeling, green; **F–J:** rabbit polyclonal anti-TGase1 antibody staining, green (FITC); **A–J:** nuclear stain, red (propidium iodide). Scale bar = 50 μm.

epidermis of the two patients with ichthyosis caused by *ABCA12* mutations, other than *TGM1* mutations, intense membrane TGase1 activity was normally observed in the upper spinous and the granular layers by pepK5 labeling (data not shown).

Immunofluorescent labeling using rabbit polyclonal anti-TGase1 antibody revealed that TGase1 immunostaining was not seen in the epidermis of Patients 1 and 2 (Figure 3, F and G). In the epidermis of Patients 3 and 4, positive immunostaining for TGase1 molecule was observed mainly in the granular layer (Figure 3, H, I, and J). From the results of pepK5 labeling and immunostaining for the TGase1 molecule, in Patients 1 and 2, it was thought that immunoreactive, intact TGase1 molecule was absent from the epidermis, resulting in the absence of FITC-pepK5 labeling. In Patients 3 and 4, although immunoreactivity for TGase1 was detected in the epidermis, FITC-pepK5 labeling was remarkably weak, suggesting reduced enzyme activity of TGase1 molecules expressed in the epidermis of these patients.

In the epidermis of any LI patient, no significant difference in pepK5 labeling pattern and intensity was seen under various experimental conditions, pH 7.4, 8.0, and 8.4, temperature 25°C, 33°C, and 37°C (data not shown).

Using FITC-conjugated pepT26 (FITC-pepT26), a preferable substrate for TGase2, only faint labeling was obtained around the granular layer cells in all of the skin samples from the patients (data not shown).

Discussion

In the first half of the present study, we examined the ability of pepK5 to detect endogenous TGase1 activity in normal human skin sections. Ca^{2+}-dependent incorporation of FITC-pepK5 into glutamine acceptor substrates was clearly seen in human epidermal keratinocytes, mainly in the upper spinous and granular layers. To date, detection of cross-linked TGase products using tissue sections has used an FITC-labeled primary amine (FITC-cadaverine) or FITC-labeled substrate peptides.[28,29] The pattern of TGase activity that we observed was consistent with that seen in the skin using FITC-cadaverine.[29] In addition, the staining sensitivity of pepK5 was remarkably higher than that of cadaverine in normal human epidermis.

As observed in immunostaining analysis, TGase1 protein localizes to the peripheral regions of the keratinocytes in the granular and upper spinous layers, consistent with previous reports.[30,31] Double fluorescence staining clearly indicated that TGase1 activity labeled with pepK5 precisely colocalized with TGase1 immunolabeling at these sites. In addition, TGase1 activity demonstrated with pepK5 overlapped with the major CCE precursor proteins, loricrin and involucrin. These findings confirm that pepK5 labeling specifically demonstrates TGase1 activity at sites of CCE formation. In the *in vitro* assay with TGase2, pepK5 reacted to a small extent at high peptide concentration.[21] Thus, in the present study,

it was necessary to check endogenous TGase2 activity in the skin samples and we confirmed that there was no significant TGase2 activity in the skin sections by FITC-labeled pepT26 labeling. From these results, we conclude that pepK5 can act as a highly sensitive and specific probe to detect *in situ* endogenous TGase1 activity in the human epidermis.

In the last half of the present study, to assess the efficacy and usefulness of pepK5 as a preferred substrate for TGase1 in evaluating TGase1 activity in LI patients, we performed *in situ* TGase1 activity assays using pepK5 as a substrate in four LI patients with *TGM1* mutations.

From the nature and sites of *TGM1* mutations in each patient and their effect on TGase1 activity, according to the protein modeling of TGase1 based on the structure of the human factor XIIIa subunit,[32] a level of remnant TGase1 activity was theoretically speculated in each case as follows.

Patient 1 is a compound heterozygote for *TGM1* nonsense mutations (Figure 2). Both nonsense mutations led to truncation of the catalytic core domain and are expected to result in a complete loss of function of TGase1 activity. Patient 2 is a homozygote for a *TGM1* deletion mutation resulting in a frameshift and premature termination in an upstream of the catalytic core domain (Figure 2). Thus, TGase1 activity is also expected to be completely abolished in the epidermis of Patient 2. In addition, all of the three truncation mutations in Patients 1 and 2 led to early termination codons. This would probably lead to complete lack of the polypeptide in the present Patients 1 and 2. Furthermore, genomic premature termination codon mutations are subject to nonsense-mediated mRNA decay resulting in mRNA degradation in some instances, depending on the mutation site.[33,34]

Patient 3 is a homozygote of a missense mutation in the center of catalytic core domain of TGase1 peptide (Figure 2). Homozygosity of this mutation is expected to result in a significant, but not complete loss of TGase1 function. Patient 4 is a compound heterozygote harboring a missense mutation in the β-sandwich domain, and the missense mutation in the center of catalytic core domain, identical to the mutation harbored by Patient 3 (Figure 2). As described above, the latter mutation in the catalytic core domain is expected to lead to a significant but only partial loss of activity of TGase1. The former mutation p.Leu204Gln in the β-sandwich domain is considered to alter protein folding, which in turn affects the protein stability of TGase 1, as suggested in other missense mutations in the β-sandwich domain.[12] This instability may result in rapid degradation of the TGase1 polypeptide and reduce TGase1 activity in the patient's epidermis, although the reduction in activity might not be as serious compared with truncation mutations in Patients 1 and 2. In addition to this simplistic view based on the position of missense mutations in the primary structure, it has been demonstrated that *TGM1* mutations in specific residues have their specific effects on the TGase1 activity, leading to specific phenotypes. For example, the distinct phenotype of self-healing collodion baby can be caused by compound heterozygous *TGM1* mutations p.Gly278Arg and p.Asp490Gly.[35] Molecular modeling and biochemical assays suggested that the high hydrostatic pressure *in utero* significantly inhibit the mutant TGase1 activity. After birth, the mutant TGase1 molecules become partially active under ordinary hydrostatic pressure, resulting in the dramatic improvement of skin symptoms in a self-healing collodion baby.[35] In addition, several *TGM1* missense mutations in specific residues were reported to cause another specific phenotype, bathing suit ichthyosis, characterized by pronounced scaling restricted to the bathing suit areas.[26,36] The affected sites are warmer body areas, and bathing suit ichthyosis is thought to be a temperature-sensitive phenotype.[26] A marked decrease of *in situ* TGase1 activity was revealed at high temperature (37°C) in the patients with bathing suit ichthyosis.[26] Recent findings have shown that wild-type TGase1 activity is clearly reduced at 25°C compared with 37°C by *in vivo* activity analysis with cadaverine as a substrate. On the other hand, in case of reconstituted mutant TGase1 molecules with the specific mutations in bathing suit ichthyosis, such as p.Arg307Gly, the TGase1 activity is increased at 33°C (and even higher at 31°C) compared with 37°C.[37] In the present study, under various temperature incubation conditions, 25°C, 33°C, and 37°C, no significant difference in the pepK5 labeling intensity was observed in normal human epidermis or in the epidermis of any LI patient, although Patient 4 had a missense mutation in Arg307 (p.Arg307Trp) in which another mutation p.Arg307Gly causing bathing suit ichthyosis phenotype was previously reported.[26] We think these discrepancies on temperature sensitivity between previous reports[26,37] and our present results may be attributable to the fact that fluorescence labeling is not completely a quantitative method. In addition, we incubated tissue sections with a substrate solution for 90 minutes in our *in situ* TGase1 activity assay. Thus, we cannot exclude the possibility that the long-time incubation might make the enzymatic reaction almost saturated and make it difficult to detect fine difference in TGase1 activity.

As the results of the present study, *in situ* TGase1 activity assays using pepK5 demonstrated a remarkably reduced or a complete lack of membrane-associated labeling in the epidermis in all patients with *TGM1* mutations compared with normal human epidermis and ichthyosis patients with *TGM1*-unrelated genetic defects. The present results indicate that pepK5 labeling can distinguish LI patients with *TGM1* mutations from normal healthy individuals and from ichthyosis patients with other causative gene mutations. In this context, specific and sensitive detection of TGase1 activity using pepK5 is thought to be a powerful tool for screening TGase1 deficiency in LI patients. Furthermore, in the present LI patients, we demonstrated that the TGase1 molecule was missing in a compound heterozygote and a homozygote for *TGM1* nonsense/truncation mutations and was present in a compound heterozygote and a homozygote for missense mutations. Accordingly, pepK5 labeling was missing in the patients with nonsense/truncation mutations, although there were weaker pepK5 signals in the patients with missense mutations. In this context, it might